The analysis of $\bar{p}p \rightarrow \pi^+\pi^-\pi^\circ\pi^\circ\pi^\circ$ in the $\pi^+\pi^-6\gamma$ Final State Part 1: $\omega\pi^\circ\pi^\circ$, $\eta\pi^\circ\pi^\circ$ and $\eta\pi^+\pi^-$

The Crystal Barrel Experiment

Curtis A. Meyer
Universität Zürich

25 September, 1992

Abstract

This document is a detailed description of the analysis of $\bar{p}p \rightarrow \pi^+\pi^-\pi^\circ\pi^\circ\pi^\circ \rightarrow \pi^+\pi^-6\gamma$. This part deals with specific intermediate states. The branching ratios for $\bar{p}p \rightarrow \omega\pi^\circ\pi^\circ$ and $\bar{p}p \rightarrow \eta\pi^\circ\pi^\circ$ are determined to be:

$$\begin{aligned} Br(\bar{p}p \rightarrow \omega\pi^\circ\pi^\circ) &= (23.98 \pm 0.59 \pm 0.75) \cdot 10^{-3} \\ Br(\bar{p}p \rightarrow \eta\pi^\circ\pi^\circ) &= (6.10 \pm 0.61 \pm 0.34) \cdot 10^{-3} \end{aligned}$$

The the branching ratio for $\bar{p}p \rightarrow \eta\pi^+\pi^-$ is also discussed, and numbers are given in the text. However, this ratio is found to be rather unstable. Finally, the $\pi^+\pi^-\pi^\circ\pi^\circ\pi^\circ$ branching ratio is estimated to be:

$$Br(\bar{p}p \rightarrow \pi^+\pi^-\pi^\circ\pi^\circ\pi^\circ) \approx 92. \cdot 10^{-3}.$$

A more detailed analalysis of this will be available in part 2 of this document.

Contents

List of Figures

1 Introduction

This document is intended to describe in detail the analysis of the $\pi^+\pi^-\pi^0\pi^0\pi^0$ final state from $\bar{p}p$ annihilation at rest. The data in this analysis come from the minimum bias data of November 1990. These data consist of approximately 3.8 million events on tape, which yield a final sample of 38,266 7–C fitted $\pi^+\pi^-\pi^0\pi^0\pi^0$ events. In this document, only the $\omega\pi\pi$ and $\eta\pi\pi$ intermediate states are discussed. The full spin parity analysis of the $\pi^+\pi^-\pi^0\pi^0\pi^0$ final state will be treated in a forthcoming CB–note, (part 2). All internally calculated numbers will normally be presented with at least two digits which are **not** significant. Only in the final numbers, will the true number of significant digits be quoted.

All errors on branching ratios are quoted as a statistical error and a systematic error. The statistical error arises solely from the statistics of the event sample. It is usually the error from MINUIT in estimating the number of events in a peak. The systematic error is composed of the following items added in quadrature:

- Any errors in branching ratios used to determine the given ratio. For example, the fact that $\omega \to \pi^+\pi^-\pi^0$ is given as 0.888 ± 0.006 is considered a systematic error.
- Any errors in absolute normalization are considered systematic.
- Any statistical errors arising from the Monte Carlo statistics are considered as systematic.

Since the first version of this paper, several changes have occured. First, all Monte Carlo samples have been increased to the point that the systematic errors are no longer significantly larger than the statistical ones. The errors sacling for the Monte Carlo has also been studied in detail, and the results are presented now. Because of this, the efficiencies have changed slightly. The numbers now presented are ceratinly the more reliable.

Second, the error scaling for real data has been carefully studied. Even though the confidence level distribution in the previous version was flat, it was clear from the pull distribution that additional work was needed. In particular, the errors on the photons were underestimated. These numbers have now been fine tuned, and I am now confident that they are good. With these new numbers, the full kinematic fitting has then been repeated. One consequence of this is that I now have about 15% more events than in the previous sample. This has caused all of the branching fractions to rise correspondingly. During this refitting, several runs were rejected due to worrisome comments in the logbook.

Finally, I have examined more carefully the $\eta\pi^+\pi^-$ final state. I am still unable to get a reliable number, but feel that I now know how to do this. However, I have not done it due to lack of time, and do not plan to do it in the near future. Instead, I present my results and conclusions to help others in extracting this branching ratio.

2 Event Selection

2.1 Skimming

The initial sample of 3,758,762 reconstructed events are first skimmed solely on information contained in the event header. An event is retained for further analysis if it satisfies the following criteria. For the charged tracks:

- There must be exactly 2 tracks connected to the found vertex. In order for a track to be connected to the primary vertex, it must either contain a PWC hit, or start no later than layer 5 in the JDC.

- Both of these tracks must be *long*. The official definition of a *long* track is that the total number of layers spanned by the track is greater than 9.
- The two tracks must be of opposite charge.
- Both tracks must have an error code smaller than 32

892,594 of the events satisfy these cuts. Assuming that all of the 3,758,762 are actually annihilations on hydrogen, that 42% of all annihilations have two prongs, and that the solid angle for two tracks described by these cuts is $0.782^2 = 0.610$, we expect that 25.6% of our data should survive. This is in good agreement with the 23.7% which actually survive.

For the crystal data:

- Only unmatched PEDs of energy larger than 20 MeV are taken.
- There must be no fewer than 6 and no more than 12 unmatched PEDs.

1,085,305 events survive these cuts, and 328,240 events survive the combination of both of these cuts. Assuming that 26% of the annihilations are $\pi^+\pi^- n\pi^0$ with $n > 2$, and that the solid angle for the detection of 6 photons is $0.97^6 = 0.833$, we expect 11.7% of the signal to remain. This is in reasonable agreement with the 8.7% which actually survive at this level. We have not considered the case when one or more photons have energy less than 20 MeV, and certainly not all events are annihilation on hydrogen. Monte Carlo studies of simple $\pi^+\pi^-\pi^0\pi^0\pi^0$ phase space events show that 8.7% of the events have at least one photon whose energy is smaller than 20 MeV.

Finally, there has been no vertex cut placed on the data. I have assumed that the use of a 7–C kinematic fit will alleviate the need for a hard vertex cut. The vertex distributions for those events which survive the skimming are shown in figure 1.

2.2 Corrections

2.2.1 Real Data

At this point, there are several known problems with the November 1990 data that need to be corrected. In reconstructing the crystals, the default vertex position was taken at ($x = 0$,$y = 0$,$z = 0$), while infact it is measured to be at ($x = 0.000$,$y = -0.224$,$z = -0.433$). This does not affect the energy of the PEDs, but does affect both θ_γ and ϕ_γ, which are corrected before proceeding with the analysis. Also, the errors on the photon quantities are underestimated. The errors used in all kinematic fitting need to be scaled as follows:

$$\begin{pmatrix} \sigma_\theta^2(1.25)^2 & \sigma_{\theta\sqrt{E}}(1.25)(1.20) & \sigma_{\theta\phi}(1.25)(1.25) \\ \sigma^2_{\sqrt{E}\theta}(1.20)(1.25) & \sigma^2_{\sqrt{E}}(1.20)^2 & \sigma_{\sqrt{E}\phi}(1.20)(1.25) \\ \sigma_{\phi\theta}(1.25)(1.25) & \sigma_{\phi\sqrt{E}}(1.25)(1.20) & \sigma_\phi^2(1.25)^2 \end{pmatrix}$$

It is also seen in these data that the momentum of all charged tracks are too small by 5 to 6%. This means that the α of all positive tracks in the **TCTR** and **TTKS** must be divided by 1.0600,

$$\alpha^+ \rightarrow \alpha^+/1.0600,$$

while the alpha of all negative tracks must be divided by 1.0500,

$$\alpha^- \rightarrow \alpha^-/1.0500.$$

Finally, the errors on several of the track quantities need to be scaled up by various factors. The 3 by 3 covariance matrix as used in all kinematic fits needs to be scaled as follows:

$$\begin{pmatrix} \sigma_\alpha^2(2.60)^2 & \sigma_{\alpha\lambda}(2.60)(1.10) & \sigma_{\alpha\psi}(2.60)(0.80)(2.00) \\ \sigma_{\lambda\alpha}(2.60)(1.10) & \sigma_\lambda^2(1.10)^2 & \sigma_{\lambda\psi}(1.10)(0.80)(2.00) \\ \sigma_{\psi\alpha}(0.80)(2.00)(2.60) & \sigma_{\psi\lambda}(2.00)(0.80)(1.10) & \sigma_\psi^2(0.80)^2(2.00)^2 \end{pmatrix}$$

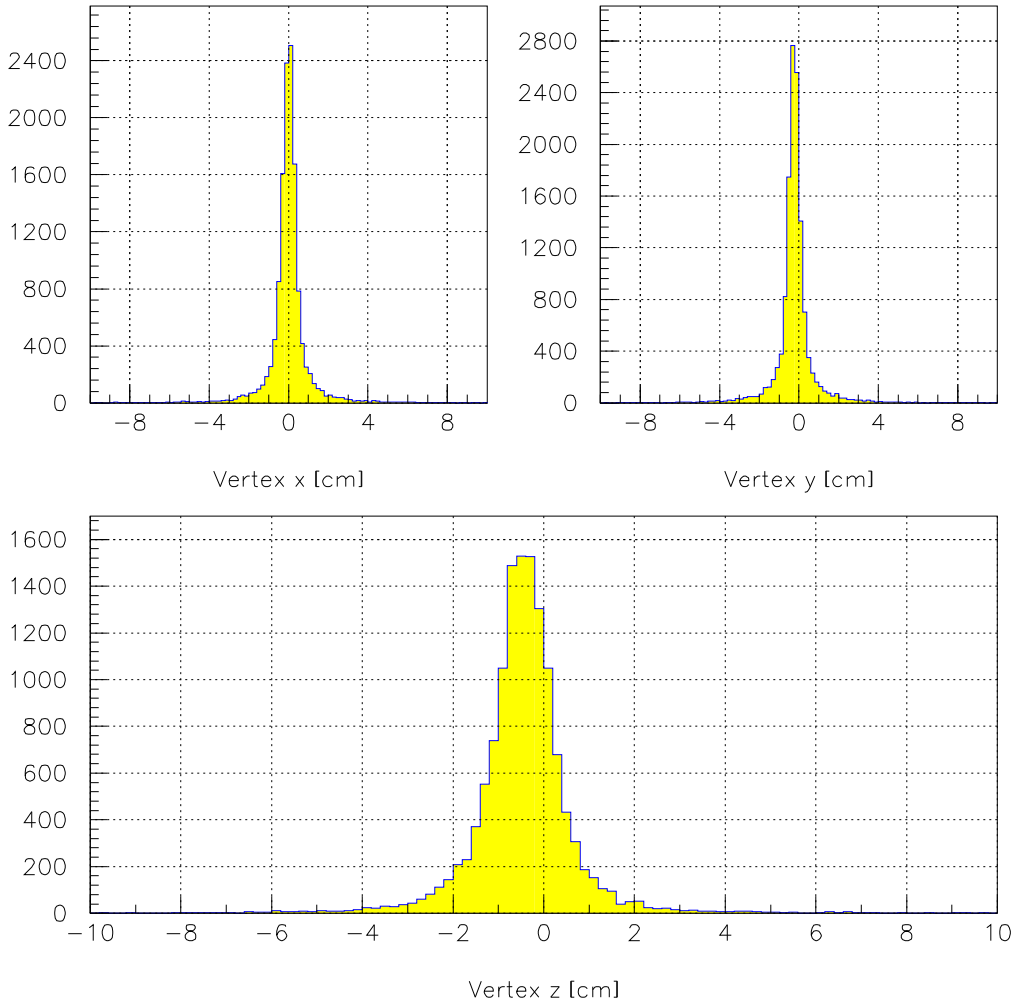

Figure 1: The vertex distribution of events which survive skimming. (UL) shows the x distribution, (UR) shows the y distribution, and (L) shows the z distribution.

2.2.2 Monte Carlo Data

Similar to real data, there are also corrections which need to be applied to any Monte Carlo Data used. The crystal errors appear to be underestimated, and need to be scaled by the following values:

$$\begin{pmatrix} \sigma_\theta^2(1.28)^2 & \sigma_{\theta\sqrt{E}}(1.28)(1.10) & \sigma_{\theta\phi}(1.28)(1.28) \\ \sigma^2_{\sqrt{E}\theta}(1.10)(1.28) & \sigma^2_{\sqrt{E}}(1.10)^2 & \sigma_{\sqrt{E}\phi}(1.10)(1.28) \\ \sigma_{\phi\theta}(1.28)(1.28) & \sigma_{\phi\sqrt{E}}(1.28)(1.10) & \sigma_\phi^2(1.28)^2 \end{pmatrix}$$

Also with the tracks, all charged momentum need to be scaled up by 5%.

$$\alpha^\pm \rightarrow \alpha^\pm/1.0500.$$

And the errors need to be tuned, but unlike the real data these factors are all rather close to one.

$$\begin{pmatrix} \sigma_\alpha^2(1.00)^2 & \sigma_{\alpha\lambda}(1.00)(0.80) & \sigma_{\alpha\psi}(1.00)(0.45)(2.00) \\ \sigma_{\lambda\alpha}(1.00)(0.80) & \sigma_\lambda^2(0.80)^2 & \sigma_{\lambda\psi}(0.80)(0.45)(2.00) \\ \sigma_{\psi\alpha}(0.45)(2.00)(1.00) & \sigma_{\psi\lambda}(0.45)(2.00)(0.80) & \sigma_\psi^2(0.45)^2(2.00)^2 \end{pmatrix}$$

2.3 Using USDROP

These 328,240 corrected events are then passed to the USDROP package [1] to locate candidates for the final state $\pi^+\pi^-6\gamma$. USDROP tries to maximize the signal in $\pi^+\pi^-6\gamma$ by never dropping additional photons if fewer than 6 would remain. An event with exactly 6 candidates would only be fit as is, while one with 7 photons would only try to drop 1, and an event with 8 photons would only try to drop 2. All events which satisfy the 4–C Confidence level from USDROP at 1% and contain exactly 6 resulting photons are retained. This sample consists of 115,985 events of these 62,936 have zero dropped, 37,394 have one dropped, and 15,655 have two dropped. 16,660 of the events have multiple solutions above 1% confidence level, however at this stage, only the most probable of these is examined. The ratio of *drop–0* to *drop–1* to *drop–2* is 4.0:2.4:1, while 14.4% of these data have more than one solution above the 1% confidence level cut.

2.4 Using CBKFIT

2.4.1 Real Data

The 115,985 events which pass USDROP are then given to CBKFIT [2], and fit to the following hypothesis:

- 4–C fit to $\pi^+\pi^-6\gamma$
- 7–C fit to $\pi^+\pi^-\pi^0\pi^0\pi^0$
- 7–C fit to $\pi^+\pi^-\eta\pi^0\pi^0$

All events which satisfy at least one of the latter two hypothesis at or above 1% confidence level are retained. This yields 68,310 events. Of these, 486 have their pile–up flag set and will be rejected at the next step. These events can be subdivided into the following samples:

- At least one $\pi^+\pi^-\pi^0\pi^0\pi^0$ 60,678 events.
- Exactly one $\pi^+\pi^-\pi^0\pi^0\pi^0$ 49,259 events, (no $\pi^+\pi^-\eta\pi^0\pi^0$).
- At least one $\pi^+\pi^-\eta\pi^0\pi^0$ 13,065 events.
- Exactly one $\pi^+\pi^-\eta\pi^0\pi^0$ 7,025 events, (no $\pi^+\pi^-\pi^0\pi^0\pi^0$).

Figure 2 shows the resulting confidence level distributions for these events. Figure 3 shows the nine pull distributions for these fits, to which Gaussians have been fit. The fit results are given in table 1.

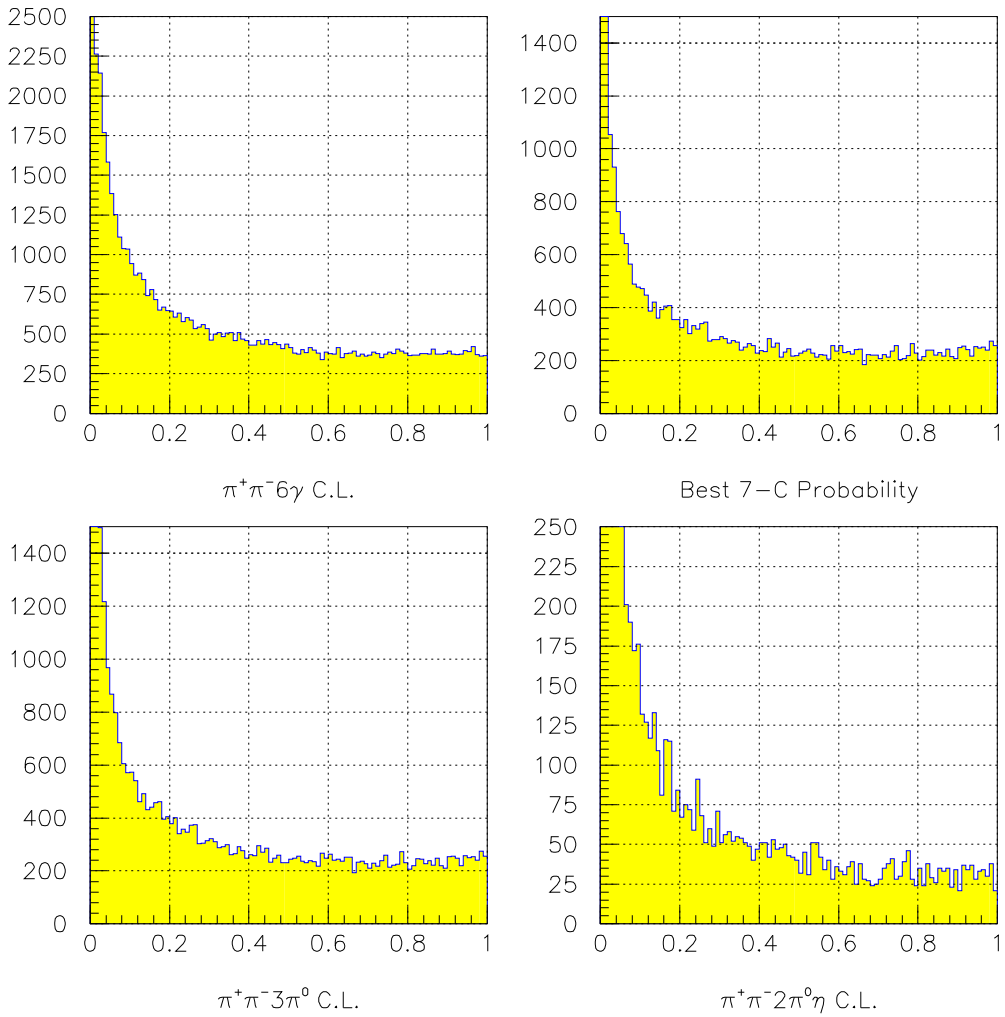

Figure 2: The 7–C confidence level distributions from CBKFIT for real data. (UL) is the 4–C distribution, (UR) is the 7–C distribution, (LL) is the $\pi^+\pi^-\pi^0\pi^0\pi^0$ and (LR) is the $\pi^+\pi^-\eta\pi^0\pi^0$

Quantity	*Mean*	*Sigma*
θ_γ	-0.0626 ± 0.0025	1.087 ± 0.0020
E_γ	0.0508 ± 0.0027	1.129 ± 0.0022
ϕ_γ	-0.0015 ± 0.0025	1.074 ± 0.0019
$1/p_{xy}^+$	-0.0182 ± 0.0066	1.105 ± 0.0049
$\tan\lambda^+$	-0.0609 ± 0.0061	1.058 ± 0.0043
ψ^+	0.0298 ± 0.0063	1.062 ± 0.0044
$1/p_{xy}^-$	0.0359 ± 0.0070	1.132 ± 0.0048
$\tan\lambda^-$	-0.0614 ± 0.0061	1.060 ± 0.0043
ψ^-	0.0176 ± 0.0063	1.075 ± 0.0044

Table 1: The fit parameters from the 7–C pulls seen in figure 3

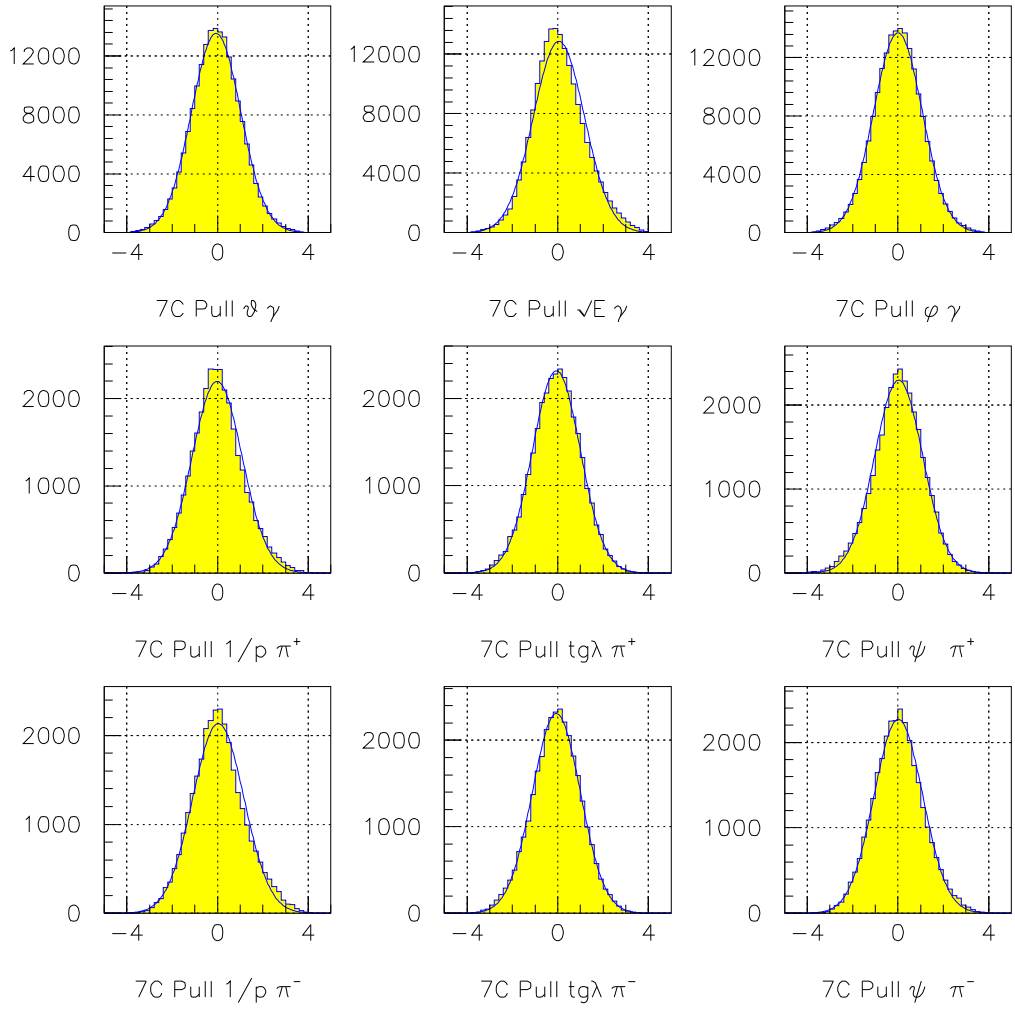

Figure 3: The pulls from the 7–C kinematic fit for real data.

2.4.2 Monte Carlo Data

In this section, the results from CBKFIT for a sample of Monte Carlo events can be compared to the real data. The sample consists of 52,500 $\pi^+\pi^-\pi^0\pi^0\pi^0$ events generatyed according to phase space. Figure 4 shows the confidence level distributions. In table 2 are summarized the fits to the pull distributions shown in Figure 5.

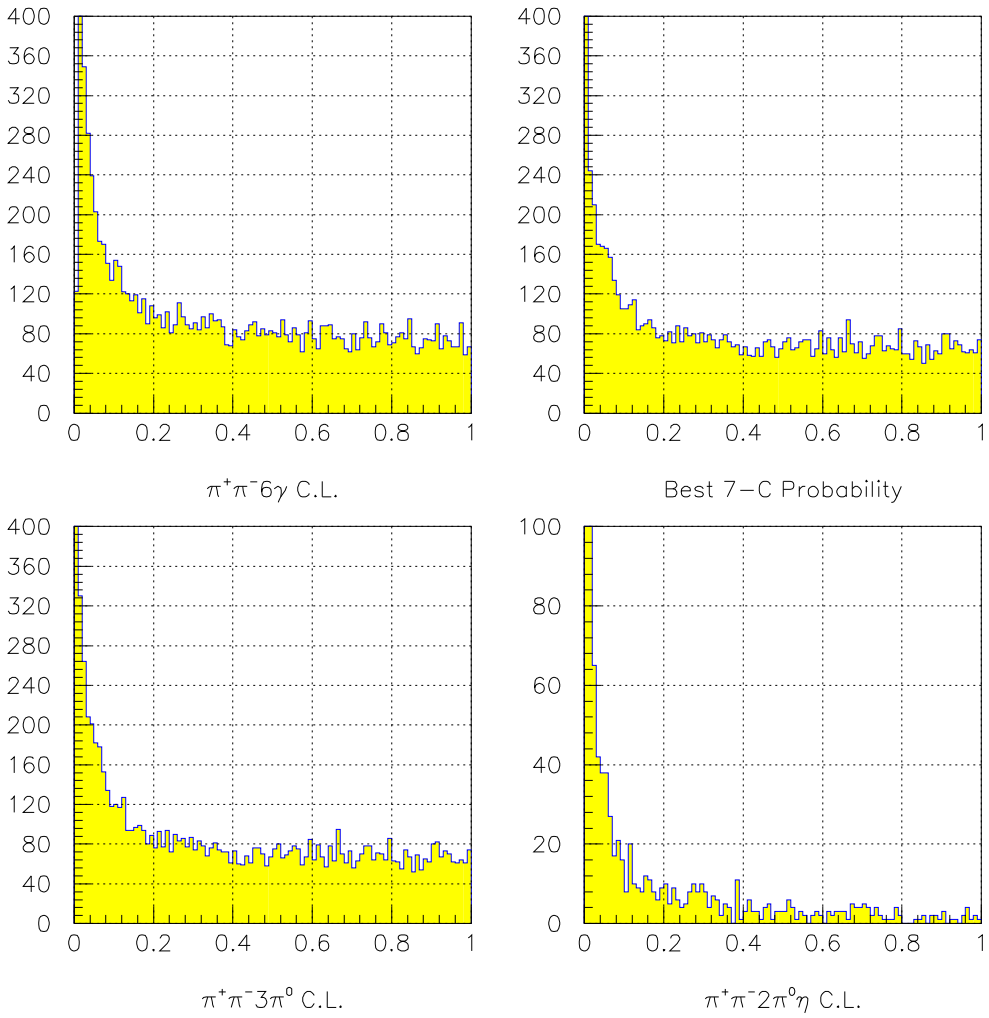

Figure 4: The 7–C confidence level distributions from CBKFIT for Monte Carlo data. (UL) is the 4–C distribution, (UR) is the 7–C distribution, (LL) is the $\pi^+\pi^-\pi^0\pi^0\pi^0$ and (LR) is the $\pi^+\pi^-\eta\pi^0\pi^0$

2.5 Definition of $\pi^+\pi^-\pi^0\pi^0\pi^0$

Of the 68,310 events from CBKFIT 60,256 have at least one $\pi^+\pi^-\pi^0\pi^0\pi^0$ solution at 1%, and no pile–up flag set. From these, it is necessary to define a $\pi^+\pi^-\pi^0\pi^0\pi^0$ sample. To do this, the event is first required to have a 7–C confidence level for $\pi^+\pi^-\pi^0\pi^0\pi^0$ larger than 15%. This reduces the event sample to 42239 events. Next, there must be no $\pi^+\pi^-\eta\pi^0\pi^0$ hypothesis with a confidence level

Quantity	*Mean*	*Sigma*
θ_γ	-0.0131 ± 0.0048	1.040 ± 0.0036
E_γ	-0.0112 ± 0.0055	1.100 ± 0.0055
ϕ_γ	0.0051 ± 0.0048	1.042 ± 0.0036
$1/p^+_{xy}$	-0.0179 ± 0.0142	1.136 ± 0.0102
$\tan\lambda^+$	-0.0066 ± 0.0146	1.044 ± 0.0083
ψ^+	0.0610 ± 0.0123	1.051 ± 0.0092
$1/p^-_{xy}$	-0.0864 ± 0.0146	1.146 ± 0.0101
$\tan\lambda^-$	-0.0069 ± 0.0121	1.068 ± 0.0087
ψ^-	-0.0932 ± 0.0117	1.017 ± 0.0087

Table 2: The fit parameters from the 7–C pulls for Monte Carlo data seen in figure 5

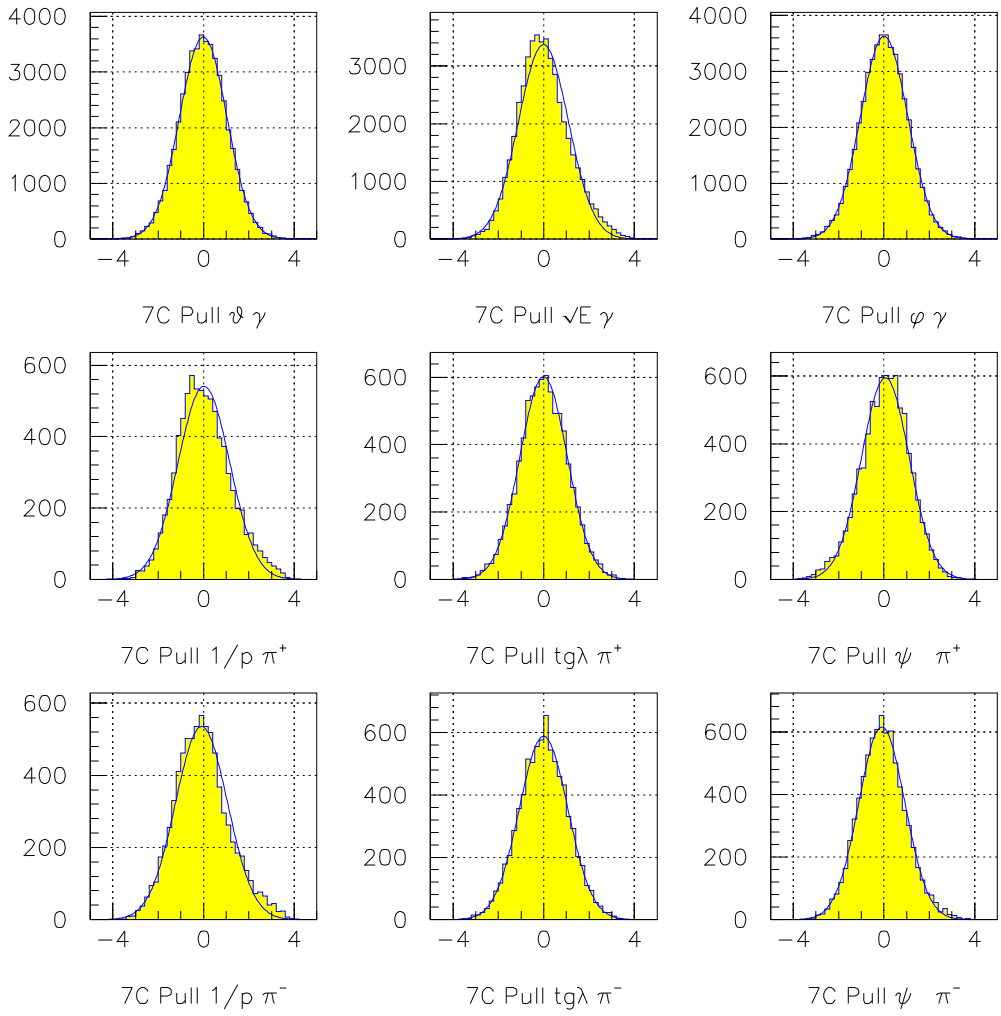

Figure 5: The pulls from the 7–C kinematic fit for real data.

larger than 1%, which leaves 38905 events. Finally, there must be no second $\pi^+\pi^-\pi^0\pi^0\pi^0$ hypothesis within 15% confidence level of the first. These cuts yield a final sample of 38,266 $\pi^+\pi^-\pi^0\pi^0\pi^0$ events, or 0.01018% of the origional 3,758,762 events.

Confidence Level	*Events*
15%	38266
25%	32172
40%	24726
50%	20395
75%	10320

Table 3: Accepted $\pi^+\pi^-\pi^0\pi^0\pi^0$ events as a function of the confidence level cut.

It is important to note that no explict vertex cut has been made anywhere in this analysis. It is assumed that the fits select only events that come from liquid hydrogen. As a demonstration of this, the vertex distributions of those events clssified as $\pi^+\pi^-\pi^0\pi^0\pi^0$ are shown in figure 6. The tails in the x, y and z distributions correspond to tracks which are nearly parallel or antiparallel. These conditions lead to singularities in the vertex fit.

2.6 The number of $\bar{p}$ stops

The initial sample of 3,758,762 events are not all $\bar{p}$ stops in liquid hydrogen. A careful treatment of this has been performed in reference [3] for the same data set. The pertainent parts of this analysis will be used here.

First, in the present analysis I effectively reject all events with the pile–up flag set. In the base sample there are 6074 events with this flag set, or 0.01615 of all events, compared to 0.0061 of the accepted events. By simply rejecting all such events, we need to scale the number of stops by 0.9838.

Annihilation outside the target is also an important consideration. This is taken from [3] as 0.961 ± 0.007. There is also an inflight contribution, which leads to an additional correction factor of 0.943 ± 0.011, (this number probably also accounts for annihilations in the iron ring as it is rather large for inflight annihilation alone).

There may finally be a residual in flight contribution to this sample. This can be accessed by looking at the assymetry in the vertex z distribution for all events accpeted for analysis. In the analysis of Burchell [3], this was found to be 0.9918 ± 0.009. Repeating his analysis for my sample, I find a value of 0.9986 ± 0.0065.

All of these corrections taken together lead to the number of stops

$$N_{stop} = 3{,}346{,}403 \pm 50{,}915,$$

(with a 1.65% systematic error in the number of stops). This number will be used in computing all branching ratios.

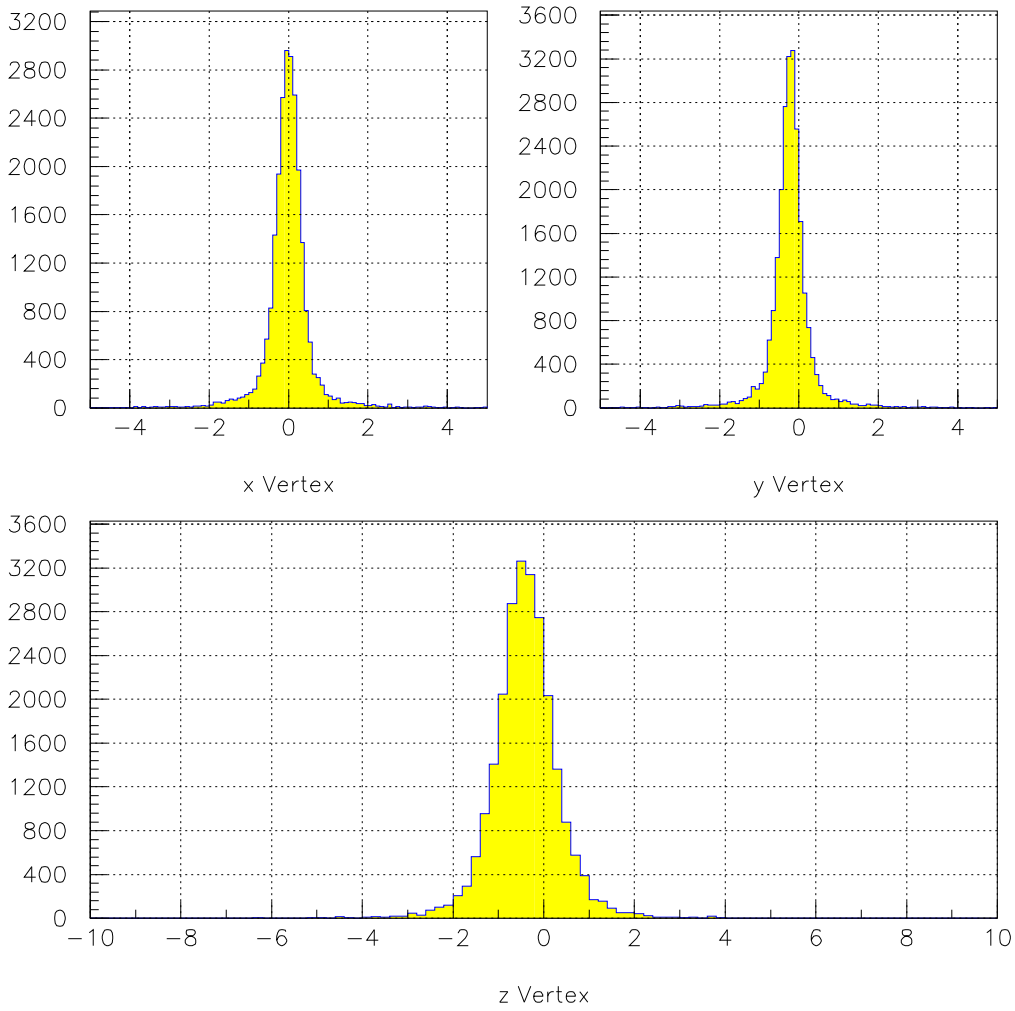

Figure 6: The vertex distribution of events defined as $\pi^+\pi^-\pi^0\pi^0\pi^0$. (UL) shows the x distribution, (UR) shows the y distribution, and (L) shows the z distribution.

3 Analysis of $\omega\pi\pi$ and $\eta\pi\pi$ into $\pi^+\pi^-\pi^\circ\pi^\circ\pi^\circ$

3.1 $\bar{p}p \to \omega\pi^\circ\pi^\circ$

3.1.1 Real Data

Identification of the ω decaying into $\pi^+\pi^-\pi^\circ$ can be seen clearly from the $\pi^+\pi^-\pi^\circ$ invariant mass spectrum, (figure 7). The inserted spectrum has been fitted using a gaussian on top of a quadratic background,

$$f(m) = A\exp(-(m-m_\omega)^2/2\sigma_\omega^2) + b_0 + b_1\cdot m + b_2\cdot m^2$$

The fit has a χ^2 of 1.157, and yields:

$$\begin{aligned} A &= 593.3 \pm 10.41 \\ m_\omega &= 783.7 \pm 0.2697 \\ \sigma_\omega &= 16.46 \pm 0.2798 \\ b_0 &= -171.6 \pm 9.040 \\ b_1 &= -0.2025 \pm 0.02202 \\ b_2 &= 0.000927 \pm 0.00001554 \end{aligned}$$

Given a bin width of 2.6667, the integral over the gaussian is computed to yield 9179.63 ± 224.26 $\omega\pi^\circ\pi^\circ$ events.

$$N_\omega = \sqrt{2\pi}\cdot\sigma_\omega\cdot(A/2.6667)$$

The reason for the mass being 2 MeV too large is at present not completely clear, but seems to be related to the momentum scaling for charged tracks. It should be noted that the mass is also high by the same amount in the Monte Carlo sample. Finally, it is not completely reasonable to treat the ω as a simple Gaussian. The natural width of the ω is 8.43 MeV, which is of similar size to the σ of the fit Gaussian. As such, these data should be fit with a Breit–Wigner convoluted with a Gaussian, (a Voigtian). Brigitt Schmid performed this analysis for the ω in her thesis [4] and showed that the Gaussian fit is equivalent, however the analysis should be repeated here.

We then define all events with an entry in the mass window 748 to 816 as possible ω's. In order to try and enhance the ω to background signal, I define:

$$\lambda = \frac{|\,\vec{p}_+ \times \vec{p}_-\,|^2}{Q^4}$$

λ can be used as a measure of the distance from the edge of the Dalitz plot to a given point in the plot. For a vector particle such as the ω, this quantity should be linear, rising from zero at $\lambda = 0$ to a maximum at $\lambda = 1$, whereas any background under the ω should be uniform over the Dalitz plot, meaning λ is constant. Figure 8 shows the distribution for all events in the ω window as well as the Dalitz plot from these events. One sees the linear structure for the true ω's on top of the constant background.

Given this sample of $\omega\pi^\circ\pi^\circ$, invariant masses and Dalitz plots are formed. These are shown in figure 9. One sees a very clear signal for the $b_1(1235) \to \omega\pi^\circ$ in both the invariant mass projection and the Dalitz plot. There is evidence as well for $f_2(1270) \to \pi^\circ\pi^\circ$, seen as an enhancement at the top of the $\pi\pi$ versus $\omega\pi$ plot, and as the rise at the high end of phase space for the $\pi^\circ\pi^\circ$ invariant mass. These agree quite well with the all–neutral analysis of $\omega\pi^\circ\pi^\circ$ performed by S. Dombrowski [5]. In figure 10 are shown these plots for restricted ranges of λ. For the high range of λ, there is a clear enhancement of signal to background, and the previous structures are clearer.

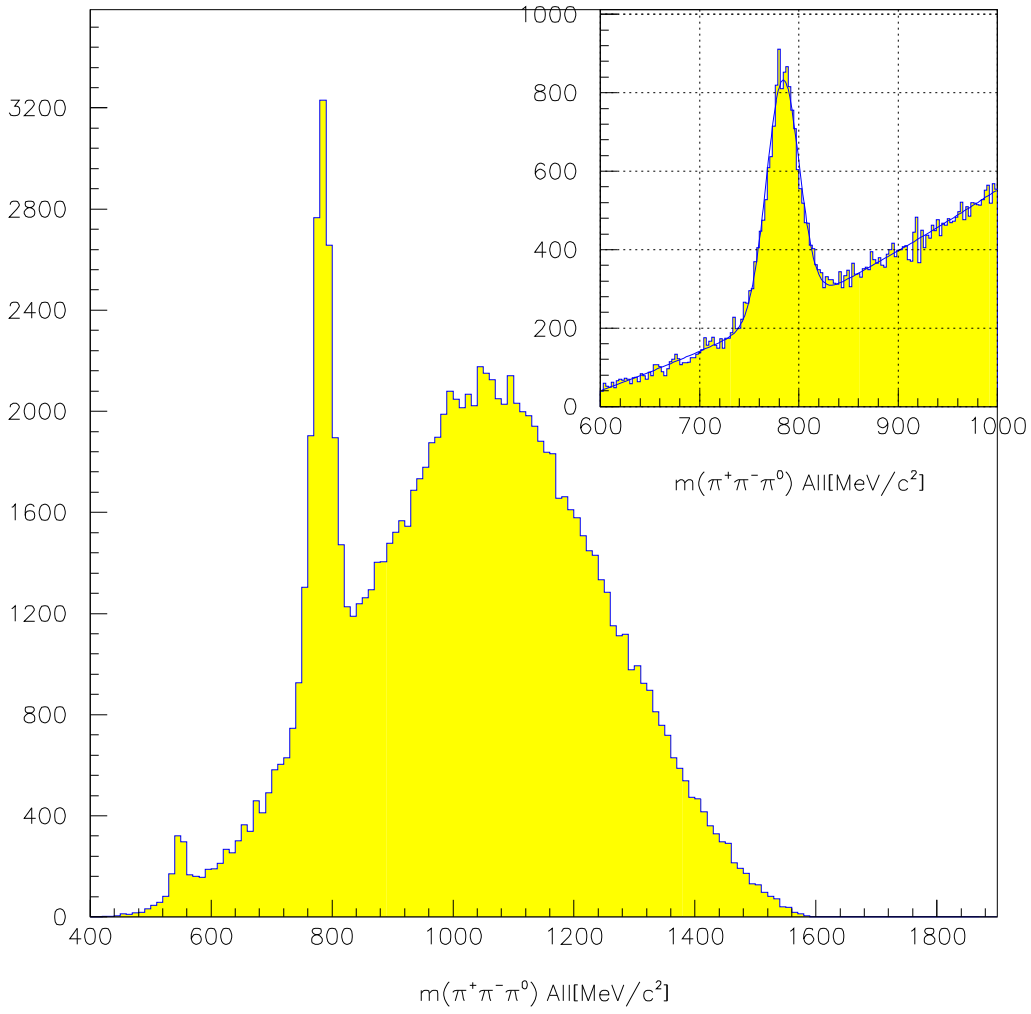

Figure 7: The $\pi^+\pi^-\pi^0$ invariant mass in 10 MeV wide bins. The inserted figure has been fit with a gaussian on a quadratic background, and has a bin width of 2.6667 MeV.

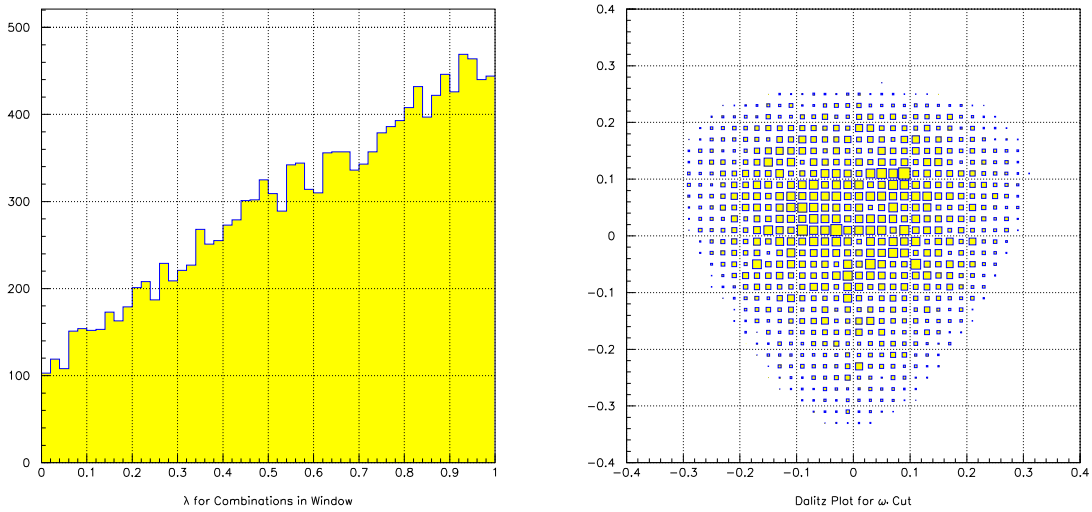

Figure 8: (L) The quantity λ for all events in the defined ω window. (R), Dalitz plot for all events in the ω window.

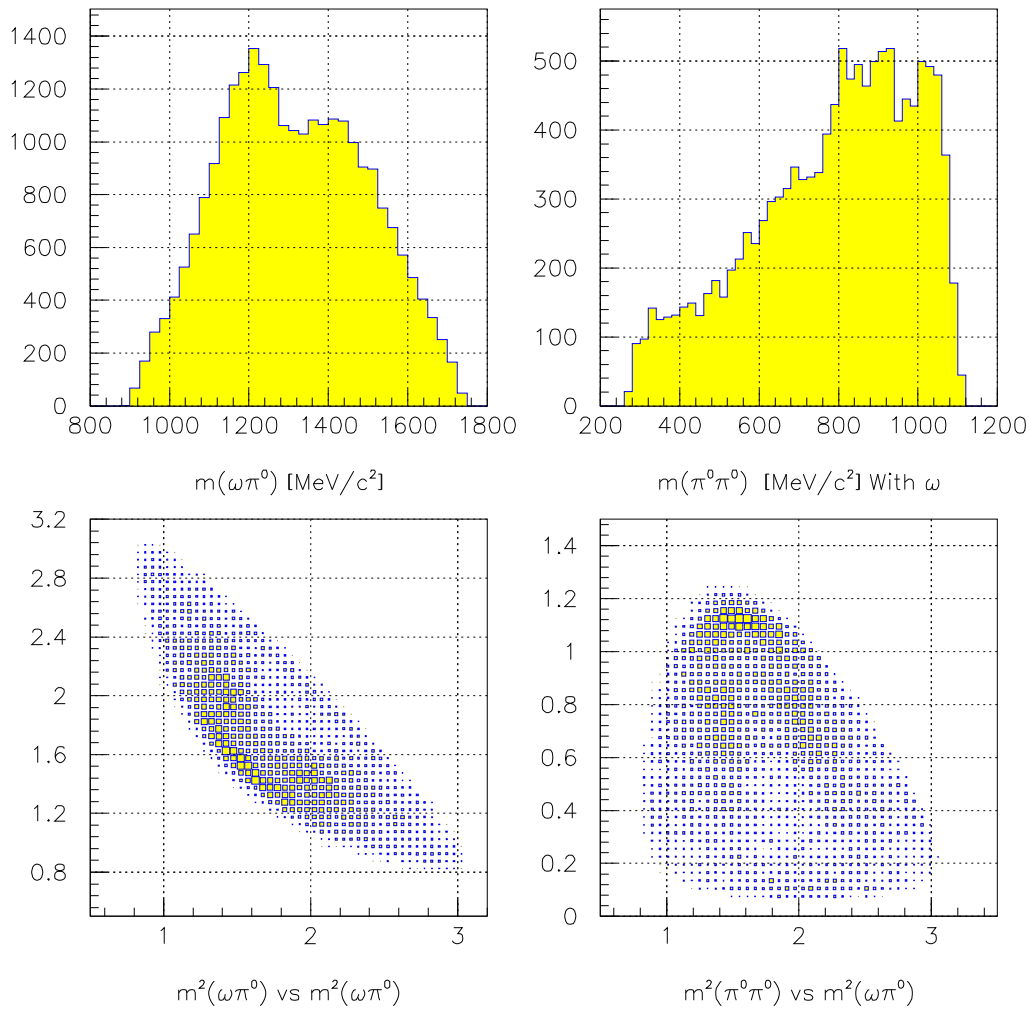

Figure 9: (UL) The invariant mass of the $\omega\pi^0$ in 10 MeV bins, (UR) the invariant mass of the $\pi^0\pi^0$ in 10 MeV bins. (LL) The Dalitz plot of $\omega\pi$ versus $\omega\pi$, (LR) The Dalitz plot of $\pi\pi$ versus $\omega\pi$.

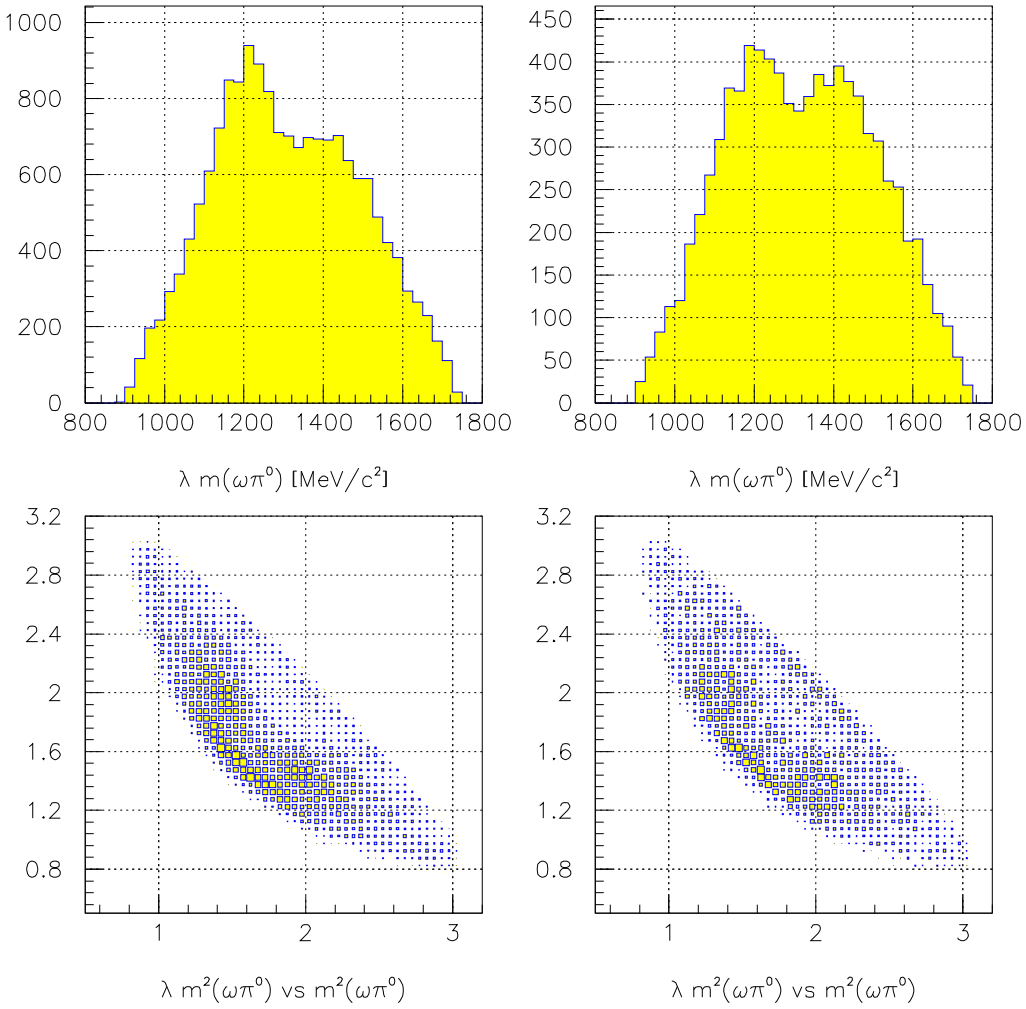

Figure 10: (UL) The invariant mass of the $\omega\pi^0$ for λ larger than 0.5 . The data are in 10 MeV bins. (UR) the invariant mass of the $\omega\pi^0$ for λ smaller than 0.5. The data are in 10 MeV bins. (LL) The Dalitz plot of $\omega\pi$ versus $\omega\pi$ for λ larger than 0.50. (LR) The Dalitz plot of $\omega\pi$ versus $\omega\pi$ for λ smaller than 0.50.

3.1.2 Monte Carlo Data

In order to estimate the efficiency for $\omega\pi^0\pi^0$, 40,717 events were generated according to phase space and run through the CBGEANT program, (version 4.06/05). The ω in these events was forced to decay 100% of the time into $\pi^+\pi^-\pi^0$, however the Dalitz decay of all 3 π^0's was allowed. The events were reconstructed and run through an identical analysis as the real data. During the skimming phase, (section 2.1), the following numbers of events were accepted:

- Two long tracks at the vertex whose charges sum to zero: 23837, (58.543%).
- Between 6 and 12 unmatched PEDs: 30288, (74.387%).
- Both of the above conditions: 17892, (43.942%).

The resulting 17892 events were then given to the USDROP package, (section 2.3). 9868 events were accepted at the 1% confidence level, of which 6131 were *drop–0*, 2727 were *drop–1* and 1010 were *drop–2*, and 823 had multiple solutions. The corresponding ratio is 6.1:2.7:1, and 8.3% of the events have multiple solutions at the 1% confidence level cut.

These events were then given to the CBKFIT code, (section 2.4).

- At least one $\pi^+\pi^-\pi^0\pi^0\pi^0$ 7,906 events.
- Exactly one $\pi^+\pi^-\pi^0\pi^0\pi^0$ 6,844 events, (no $\pi^+\pi^-\eta\pi^0\pi^0$).
- At least one $\pi^+\pi^-\eta\pi^0\pi^0$ 667 events.
- Exactly one $\pi^+\pi^-\eta\pi^0\pi^0$ 75 events, (no $\pi^+\pi^-\pi^0\pi^0\pi^0$).

Of these, 5,456 satisfied the definition of $\pi^+\pi^-\pi^0\pi^0\pi^0$, (section 2.5). These events were then passed through the ω analysis, (section 3.1.1), and the resulting $\pi^+\pi^-\pi^0$ invariant mass is shown in figure 11. This is fit to a Gaussian plus quadratic background. The resulting fit has a χ^2 of 1.114, and yields:

$$\begin{aligned} A &= 445.5 \pm 8.828 \\ m_\omega &= 783.7 \pm 0.2103 \\ \sigma_\omega &= 12.44 \pm 0.1913 \\ b_0 &= -251.2 \pm 3.891 \\ b_1 &= 0.6488 \pm 0.009368 \\ b_2 &= -0.0003538 \pm 0.000006384 \end{aligned}$$

which when integrated gives 5209.42 ± 130.67, and an efficiency for reconstruction of 0.127942 ± 0.003209.

In order to determine if the presence of intermediate resonances can affect this efficiency, it is necessary to evaluate the efficiency for $b_1(1235)\pi^0$ and $f_2(1270)\omega$. To do this, it is not necessary to generate new Monte Carlo data. Rather, we can examine all of the produced $\omega\pi^0\pi^0$ events, and assign a dynamical weight based on a Breit–Wiger function of the resulting mesons. We can then take the sum of these weights in the entire generated sample, and the sum of these weights for those events accepted by the analysis. The ratio of these will be the efficiency for the given channel. If n_a sums over accepted events, and n_g sums over generated events, the ratio is:

$$\epsilon_{res} = \frac{\sum_i^{n_a} w(e_i)}{\sum_j^{n_g} w(e_j)}$$

In this analysis, we define the number of events as those that satisfy the definition of $\pi^+\pi^-\pi^0\pi^0\pi^0$, and not the number from the fit. For this reason, the phase space efficiency is 0.133998 and not

0.127942, (a factor 0f 1.04733 larger). The results are shown in table 4. We see that the presence of an intermediate resonance tends to increase the efficiency. If we assume we know nothing about such resonances, the most sensible value to take is the simple average of all numbers in the table. This then gives an efficiency of 0.134909 ± 0.001070, where the error is the standard deviation of the efficiencies. This error is treated as an additional systematic error, and added in quadrature with the previous error to the efficiency, (0.003209). Rescaling this back to the fit value, and including the additional systematic error yields 0.128812 ± 0.003388.

Decay Chain	*Generated*	*Accepted*	*Efficiency*
$\omega\pi^0\pi^0$ Phase Space	40717	5456	0.133998
$b_1(1235)\pi^0 \rightarrow (\omega\pi^0)\pi^0$	12112	1648.8	0.136088
$\omega f_2(1270) \rightarrow \omega(\pi^0\pi^0)$	2383.3	320.89	0.134641
Average			0.134909 ± 0.001070

Table 4: The efficiency for reconstructing $\omega\pi^0\pi^0$ for the allowed intermediate states.

.

Can we understand this apparently low efficiency? Given only the solid angle effects, we estimated in section 2.1 that each track has a 78.2% detection efficiency and each photon has a 97% detection efficiency. The product then yields:

$$\epsilon_\Omega = (0.782)^2 \cdot (0.97)^6 = 0.509$$

and including the Dalitz decays, ($\epsilon_d = 0.98798$ per π^0), would reduce this to 0.494. We have also placed a 15% Confidence level cut, ($\epsilon_{cl} = 0.850$), which brings us down to 0.420. Now recall that in the $3\pi^0$ analysis [7] that the total reconstruction efficiency was 30% using a 10% confidence level cut. From this we can estimate that in a split–off free environment, after simple photon solid angle effects have been unfolded, the chance of reconstructing a single π^0 is about 74%.

$$\epsilon_{\pi^\circ} = \left(\frac{0.30}{0.90 \cdot (0.97)^6}\right)^{1/3} = 0.74$$

Using this, we have:

$$\epsilon_\omega = \epsilon_\Omega \cdot \epsilon_{\pi^\circ}^3 \cdot (\epsilon_d)^3 \cdot \epsilon_{cl} = 0.167$$

At this point, it is not hard to imagine that the inclusion of charged particles and their associated split–off problems could account for the remaining 4%, and in this sense, the computed efficiency of 12.88% is understandable.

3.1.3 Branching Fraction

We have $N_\omega = 9179.63 \pm 224.26$ $\omega\pi^0\pi^0$ events, and take the branching ratio for $\omega \rightarrow \pi^+\pi^-\pi^0$ as $b_\omega = 0.888 \pm 0.006$ [6]. The total number of $\bar{p}$ stops is $N_{stop} = 3{,}346{,}403 \pm 50{,}915$ (section 2.6), and the efficiency for reconstruction of an ω is $\epsilon_\omega = 0.128812 \pm 0.003388$. Then the branching ratio, f_b is given as:

$$f_b = \frac{N_\omega}{N_{stop} \cdot b_\omega \cdot \epsilon_\omega},$$

yielding:

$$BR(\bar{p}p \rightarrow \omega\pi^0\pi^0) = (23.98 \pm 0.59 \pm 0.75) \cdot 10^{-3},$$

where the first error is statistical and the second is systematic.

We now wish to access the effects of the confidence level cut on this result. The entire analysis has been repeated using a 25% and 50% cut in the 7–C confidence level. The results of these analysis are shown as the ratio of accepted event to Monte Carlo efficiency in table 5. All three results are identical. This branching ratio is then considered as a good measurement.

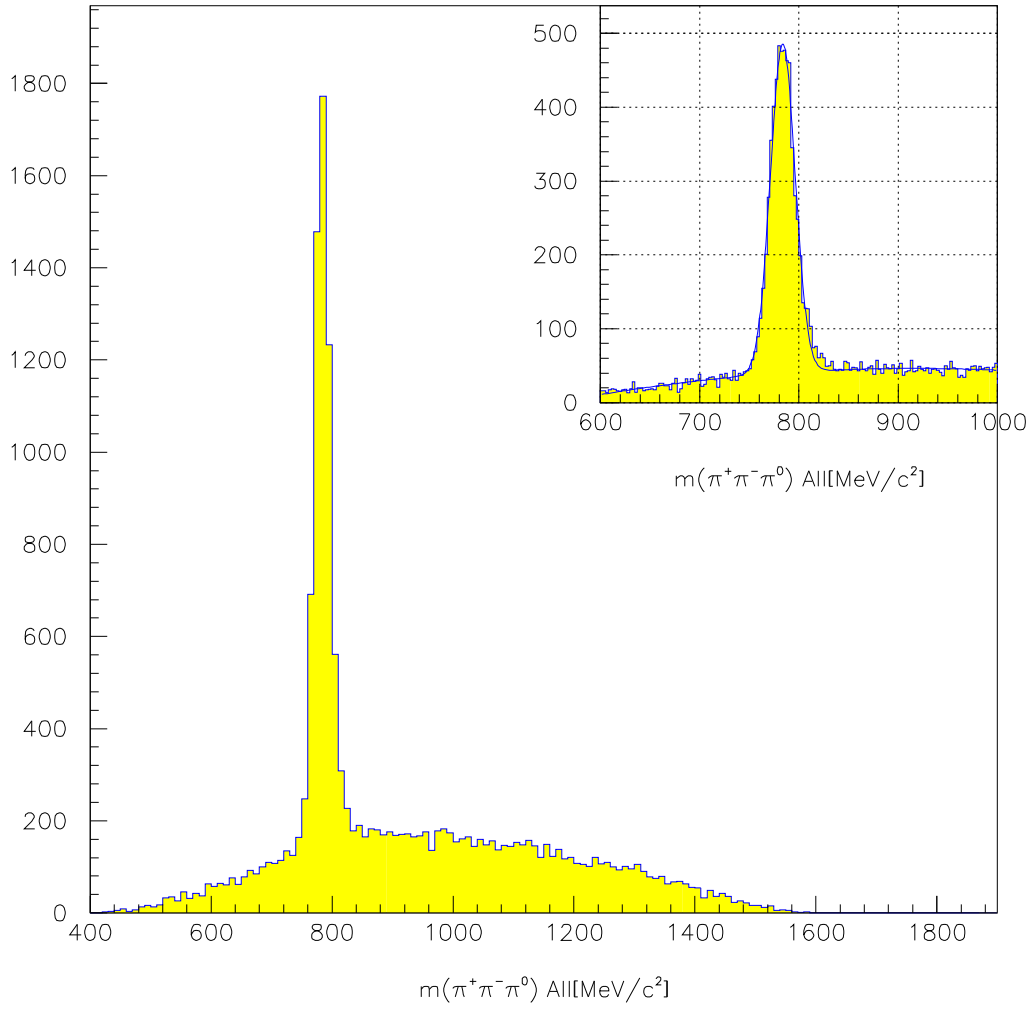

Figure 11: The Monte Carlo $\pi^+\pi^-\pi^0$ invariant mass. The inserted figure has been fit with a gaussian on a quadratic background.

Confidence Level	*Acc. Events*	*M.C. eff.*	*Ratio*
15%	9179.63 ± 224.26	0.127942 ± 0.003209	71748 ± 2512
25%	7905.47 ± 206.20	0.110809 ± 0.002946	71343 ± 2657
40%	6204.89 ± 180.81		
50%	5205.59 ± 162.07	0.073349 ± 0.002360	70970 ± 3177
75%	2612.32 ± 118.23		
χ^2 for 3 d.f.			0.0390

Table 5: The number of $\omega\pi^0\pi^0$ as a function of the 7–C confidence level

3.2 $\bar{p}p \to \eta\pi^0\pi^0$

3.2.1 Real Data

Identification of the η decaying into $\pi^+\pi^-\pi^0$ can be seen clearly from the $\pi^+\pi^-\pi^0$ invariant mass spectrum, (figure 12). The inserted spectrum has been fitted using a gaussian on top of a quadratic background,

$$f(m) = A\exp(-(m-m_\eta)^2/2\sigma_\eta^2) + b_0 + b_1 \cdot m + b_2 \cdot m^2$$

The fit has a χ^2 of 0.8687, and yields:

$$\begin{aligned} A &= 83.48 \pm 5.835 \\ m_\eta &= 547.9 \pm 0.5884 \\ \sigma_\eta &= 9.237 \pm 0.6329 \\ b_0 &= 378.7 \pm 4.270 \\ b_1 &= -1.770 \pm 0.01384 \\ b_2 &= 0.002072 \pm 0.00001646 \end{aligned}$$

Given a bin width of 3.33333, the integral over the gaussian in the first case gives 581.69 ± 58.20 $\eta\pi^0\pi^0$ events.

If we now define an η window as 526 MeV to 580 Mev, we can form the $\eta\pi\pi$ Dalitz plot, (figure 13). Examining figure 12, it is clear that about 50% of the events in the η window are in fact background events. As such, the fact that these plots do not look the same as seen in the all–neutral analysis of $\eta\pi^0\pi^0$ should not be overly alarming. Looking in the $\pi^0\pi^0$ plot, we do see a structure near 1300 MeV which may be the $f_2(1270)$. An explanation of the structure in the $\eta\pi$ invariant mass is not attempted.

3.2.2 Monte Carlo Data

In order to estimate the efficiency for $\eta\pi^0\pi^0$, 17,102 events were generated according to phase space and run through the CBGEANT program, (version 4.06/06). The η in these events was forced to decay 100% of the time into $\pi^+\pi^-\pi^0$, however the Dalitz decay of all π^0's was allowed. The events were reconstructed and run through an identical analysis as the real data. During the skimming phase, (section 2.1), the following numbers of events were accepted:

- Two long tracks at the vertex whose charges sum to zero: 9589, (56.069%).
- Between 6 and 12 unmatched PEDs: 12318, (72.027%).
- Both of the above conditions: 7013, (41.007%).

The resulting 7013 events were then given to the USDROP package, (section 2.3). 4037 events were accepted at the 1% confidence level, of which 2732 were *drop–0*, 979 were *drop–1* and 326 were *drop–2*, and 366 had multiple solutions. The corresponding ratio is 8.3:3.0:1, and 9.07% of the events have multiple solutions at the 1% confidence level cut.

These events were then given to the CBKFIT code, (section 2.4).

- At least one $\pi^+\pi^-\pi^0\pi^0\pi^0$ 3,191 events.
- Exactly one $\pi^+\pi^-\pi^0\pi^0\pi^0$ 2,738 events, (no $\pi^+\pi^-\eta\pi^0\pi^0$).
- At least one $\pi^+\pi^-\eta\pi^0\pi^0$ 319 events.
- Exactly one $\pi^+\pi^-\eta\pi^0\pi^0$ 32 events, (no $\pi^+\pi^-\pi^0\pi^0\pi^0$).

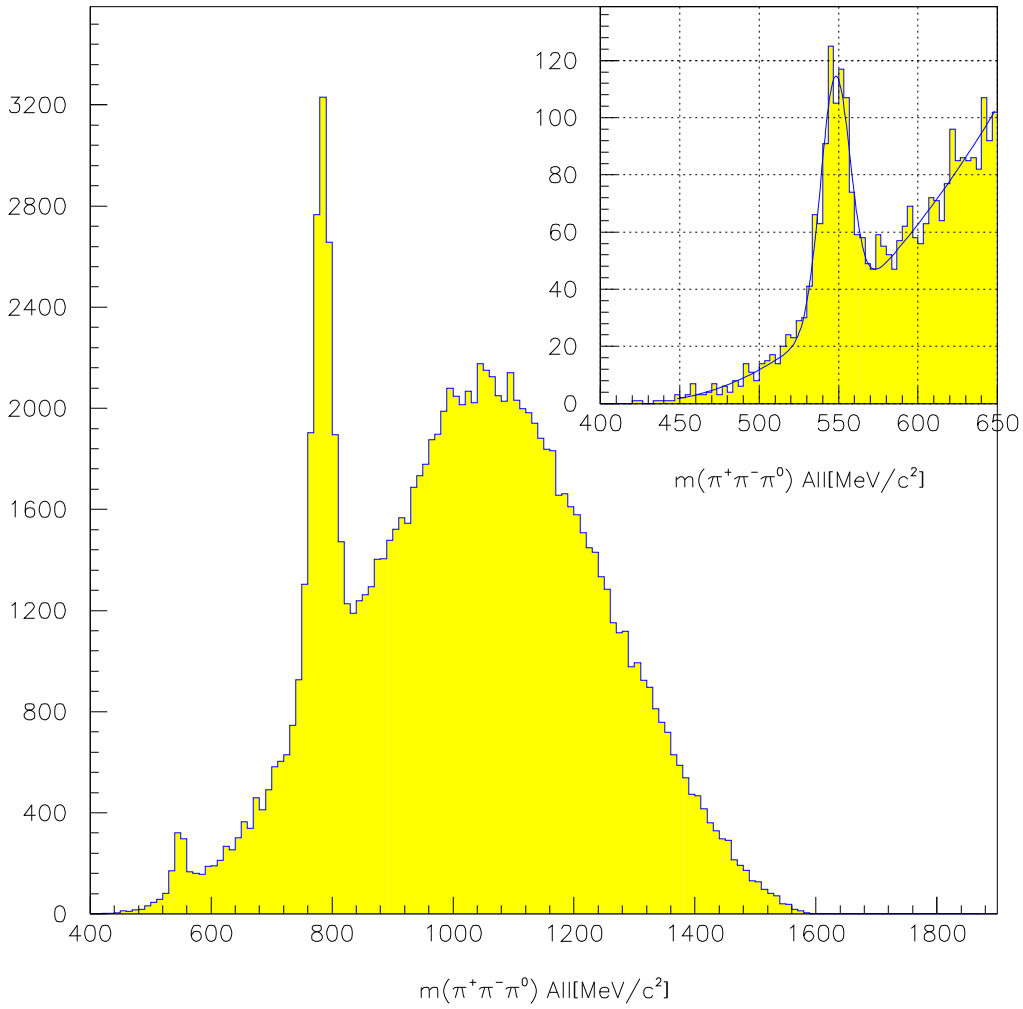

Figure 12: The $\pi^+\pi^-\pi^0$ invariant mass in 10 MeV bins. The inserted figure has been fit with a gaussian on a quadratic background, and has a bin width of 3.333 MeV.

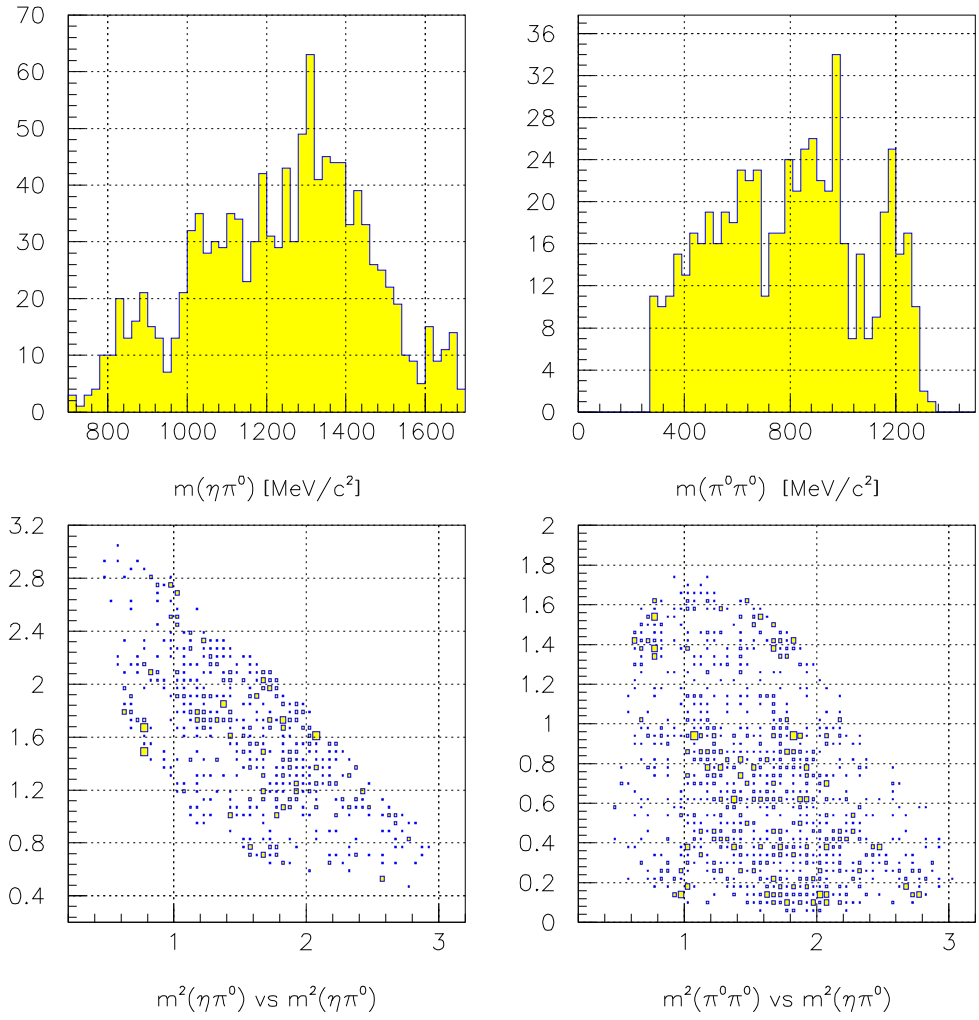

Figure 13: (UL) The $\eta\pi^0$ invariant mass plot in 10 MeV bins, (two entries per event). (UR) The $\pi^0\pi^0$ invariant mass in 15 MeV bins, (one entry per event). (LL) The Dalitz plot of $\eta\pi^0$ versus $\eta\pi^0$, (two entries per event. (LR) The Dalitz plot of $\pi^0\pi^0$ versus $\eta\pi^0$, (two entries per event).

Of these, 2146 satisfied the definition of $\pi^+\pi^-\pi^0\pi^0\pi^0$, (section 2.5). These events were then passed through the η analysis, (section 3.2.1), and the resulting $\pi^+\pi^-\pi^0$ invariant mass is shown in figure 14. This is fit to a Gaussian plus quadratic background. The resulting fit has a χ^2 of 1.120, and yields:

$$\begin{aligned} A &= 366.9 \pm 11.21 \\ m_\eta &= 549.8 \pm 0.2751 \\ \sigma_\eta &= 7.404 \pm 0.1581 \\ b_0 &= -22.61 \pm 2.352 \\ b_1 &= 0.03988 \pm 0.008116 \\ b_2 &= -0.00002964 \pm 0.000008903 \end{aligned}$$

which when integrated with a bin width of 3.33333, these yield 2042.80 ± 76.15. This leads to a reconstruction efficiency of 0.119448 ± 0.004452.

In order to access the effect of intermediate resonances, an analysis as in section 3.1.2 has been carried out. The results are shown in table 6. As before, we will normalize to the average of all intermediate resonances, and the the standard deviation of those values into the systematic error in the efficiency. This then yields: $\epsilon_\eta = 0.120712 \pm 0.005731$.

Decay Chain	*Generated*	*Accepted*	*Efficiency*
$\eta\pi^0\pi^0$ Phase Space	17102	2146	0.125482
$\eta f_0(975) \rightarrow \eta(\pi^0\pi^0)$	1090.4	139.28	0.127733
$\eta f_2(1270) \rightarrow \eta(\pi^0\pi^0)$	2895.1	390.70	0.134952
$a_0(980)\pi^0 \rightarrow (\eta\pi^0)\pi^0$	1559.7	197.50	0.126627
$a_2(1320)\pi^0 \rightarrow (\eta\pi^0)\pi^0$	3302.1	431.36	0.130632
Average			$.129085 \pm 0.003797$

Table 6: The efficiency for reconstructing $\eta\pi^0\pi^0$ for the allowed intermediate states.

.

3.2.3 Branching Fraction

We have $N_\eta = 581.69 \pm 58.20$ $\eta\pi^0\pi^0$ events, and take the branching ratio for $\eta \rightarrow \pi^+\pi^-\pi^0$ as $b_\eta = 0.236 \pm 0.006$ [6]. The total number of $\bar{p}$ stops is $N_{stop} = 3{,}346{,}403 \pm 50{,}915$ (section 2.6), and the efficiency for reconstruction of an η is $\epsilon_\eta = 0.120712 \pm 0.005731$. Then the branching ratio, f_b is given as:

$$f_b = \frac{N_\eta}{N_{stop} \cdot b_\eta \cdot \epsilon_\eta}.$$

This then yields that

$$BR(\bar{p}p \rightarrow \eta\pi^0\pi^0) = (6.10 \pm 0.61 \pm 0.34) \cdot 10^{-3}.$$

where the first error is statistical and the second is systematic.

I have also varied the confidence level cut, and repeated the above analysis for 25% and 50% cuts. The results shown in table 7 show no systematic shifts with the rising confidence level cut. As such, this branching ratio is considered a good measurement.

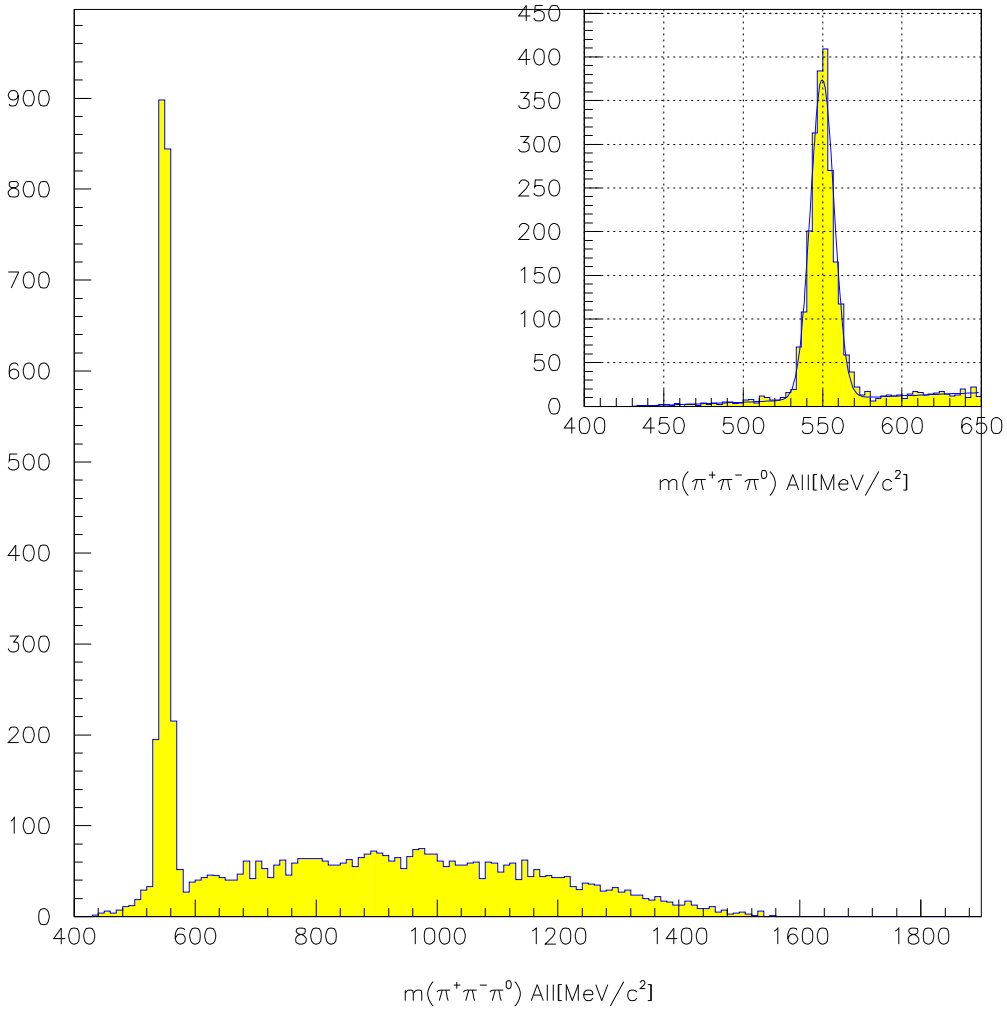

Figure 14: The Monte Carlo $\pi^+\pi^-\pi^0$ invariant mass. The inserted figure has been fit with a gaussian on a quadratic background.

Confidence Level	*Acc. Events*	*M.C. eff.*	*Ratio*
15%	581.69 ± 58.20	0.119448 ± 0.004452	4870 ± 520
25%	511.44 ± 52.72	0.102222 ± 0.004093	5003 ± 553
40%	357.24 ± 44.61		
50%	296.09 ± 40.65	0.065745 ± 0.003312	4504 ± 659
75%	153.83 ± 31.86		
χ^2 for 3 d.f.			0.3484

Table 7: The number of $\eta\pi^0\pi^0$ as a function of the 7–C confidence level

3.3 $\bar{p}p \to \eta\pi^+\pi^-$

3.3.1 Real Data

Identification of the η decaying into $\pi^0\pi^0\pi^0$ can be seen clearly from the $\pi^0\pi^0\pi^0$ invariant mass spectrum, (figure 15). Unfortunately, using this $3\pi^0$ invariant mass to determine a branching fraction leads to inconssistent results. These seem to arise from the large likelyhood to find more than one way to form the π^0's from the η decay. Inorder to try avoid this pitfall, these data have been analyzed using the 4–C fit results rather than the 7–C results as in the previous two sections. Unfortunately, the 4–C fit was simply that in USDROP, rather than a proper treatment using CBKFIT. An alternate approach would also be to perform an 8–C fit by adding the $\eta \to 3\pi^0$ decay as a constraint. This has not been done.

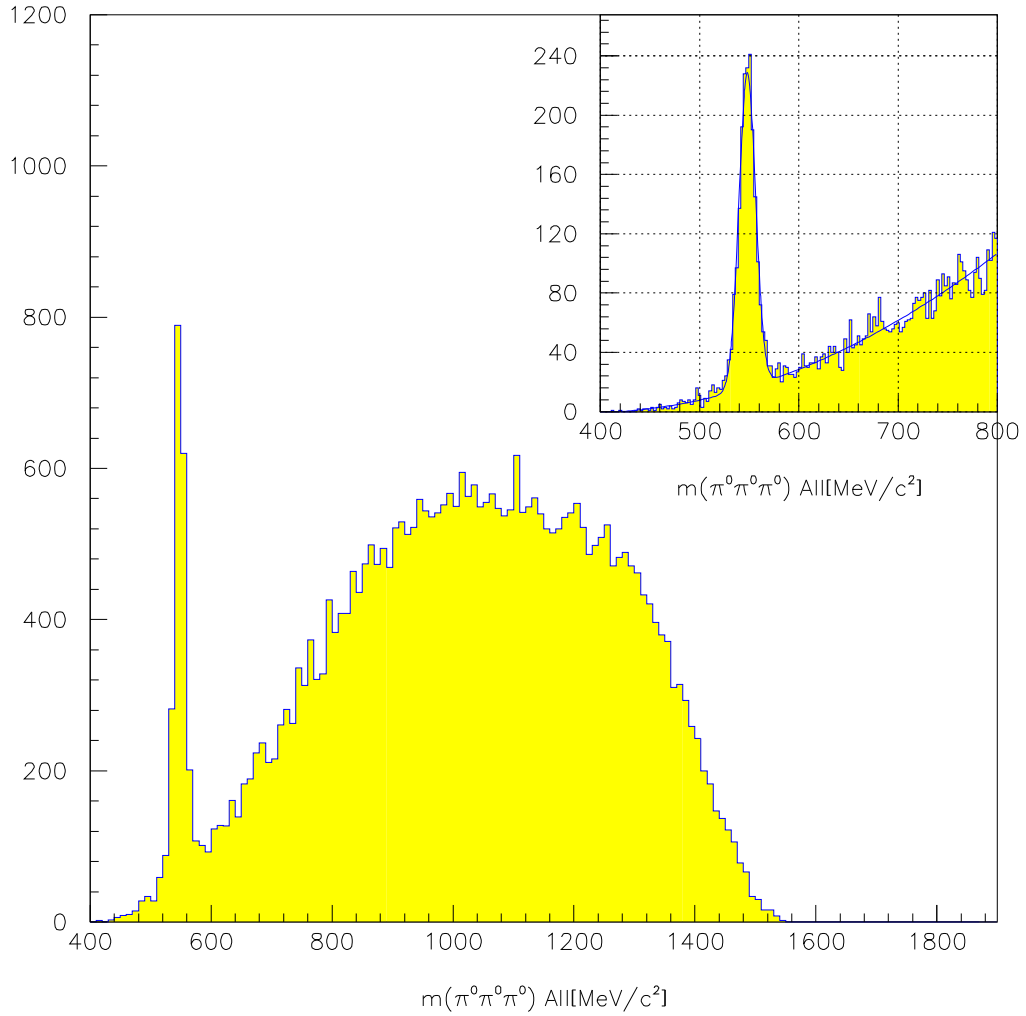

Figure 15: The $\pi^0\pi^0\pi^0$ invariant mass in 10 MeV bins. The inserted figure has been fit with a gaussian on a quadratic background, and has a bin width of 2.6667 MeV.

Using an analysis identical to the previous sections, and fitting the $3\pi^0$ invariant mass of figure 15,

we obtain:

$$\begin{aligned} A &= 212.5 \pm 7.519 \\ m_\eta &= 548.0 \pm 0.2401 \\ \sigma_\eta &= 8.345 \pm 0.2317 \\ b_0 &= 88.51 \pm 2.252 \\ b_1 &= -0.4688 \pm 0.007861 \\ b_2 &= 0.0006147 \pm 0.000007625 \end{aligned}$$

Given a bin width of 2.6667, the integral over the gaussian gives 1666.89 ± 72.65 events.

If we now define an η window as 532 MeV to 564 Mev of figure 15, we can form the $\eta\pi\pi$ Dalitz plot, (figure 16). In the $\pi^+\pi^-$ invariant mass, a very clear signal is seen for the ρ^0. We also see a structure near 1300 MeV which may or may not be the $f_2(1270)$. Finally, there may be a structure near 950 MeV which could be the $f_0(975)$. The structure in the $\eta\pi$ mass is not so easily disentangled.

In the modified analysis, the 6γ invariant mass was formed for all events having a 4–C confidence level larger than 25%. This yielded a sample of 62,006 events whose invariant mass spectra is shown in figure 17. The inserted spectrum has been fitted using a Gaussian on top of a quadratic background,

$$f(m) = A\exp(-(m-m_\eta)^2/2\sigma_\eta^2) + b_0 + b_1 \cdot m + b_2 \cdot m^2$$

The fit to figure 17 has a χ^2 of 1.057, and yields:

$$\begin{aligned} A &= 142.7 \pm 5.496 \\ m_\eta &= 552.1 \pm 0.4410 \\ \sigma_\eta &= 12.94 \pm 0.4601 \\ b_0 &= 49.32 \pm 3.260 \\ b_1 &= -0.3777 \pm 0.01169 \\ b_2 &= 0.0006452 \pm 0.0000111 \end{aligned}$$

Given a bin width of 2.6667, the integral over the gaussian gives 1735.72 ± 90.98 events.

3.3.2 Monte Carlo Data

In order to estimate the efficiency for $\eta\pi^+\pi^-$, 30,000 events were generated according to phase space and run through the CBGEANT program, (version 4.06/06). The η in these events was forced to decay 100% of the time into $3\pi^0$'s, however the Dalitz decay of all 3 π^0's was allowed. The events were reconstructed and run through an identical analysis as the real data. During the skimming phase, (section 2.1), the following numbers of events were accepted:

- Two long tracks at the vertex whose charges sum to zero: 18,542, (61.81%).
- Between 6 and 12 unmatched PEDs: 22,582, (75.27%).
- Both of the above conditions: 14,025, (46.75%).

The resulting 14,025 events were then given to the USDROP package, (section 2.3). 7734 events were accepted at the 1% confidence level, of which 4137 were *drop–0*, 2555 were *drop–1* and 1042 were *drop–2*, and 1083 had multiple solutions. The corresponding ratio is 4.0:2.5:1, and 14.0% of the events have multiple solutions at the 1% confidence level cut.

These events were then given to the CBKFIT code, (section 2.4).

- At least one $\pi^+\pi^-\pi^0\pi^0\pi^0$ 5,485 events.

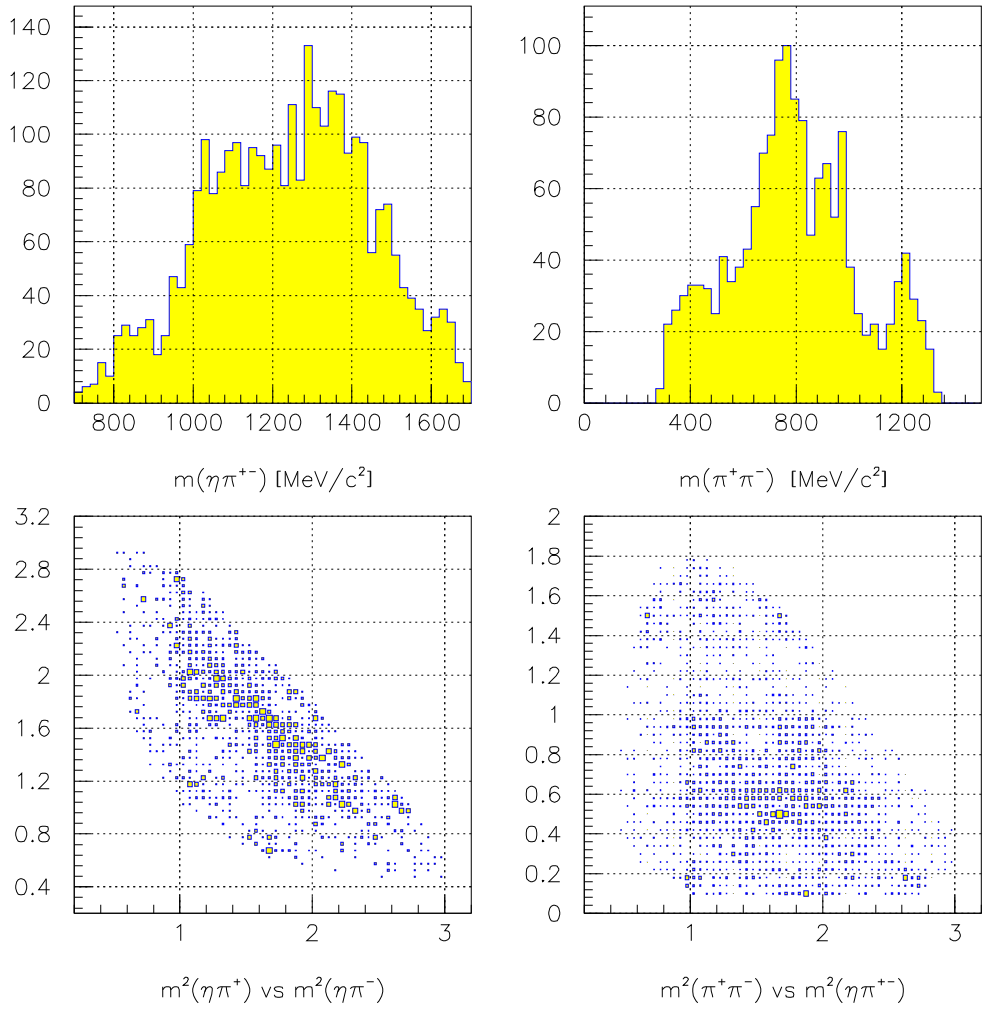

Figure 16: (UL) The $\eta\pi^{\pm}$ invariant mass plot in 10 MeV bins, (two entries per event). (UR) The $\pi^+\pi^-$ invariant mass in 15 MeV bins, (one entry per event). (LL) The Dalitz plot of $\eta\pi^{\pm}$ versus $\eta\pi^{\mp}$, (two entries per event. (LR) The Dalitz plot of $\pi^+\pi^-$ versus $\eta\pi^{\pm}$, (two entries per event).

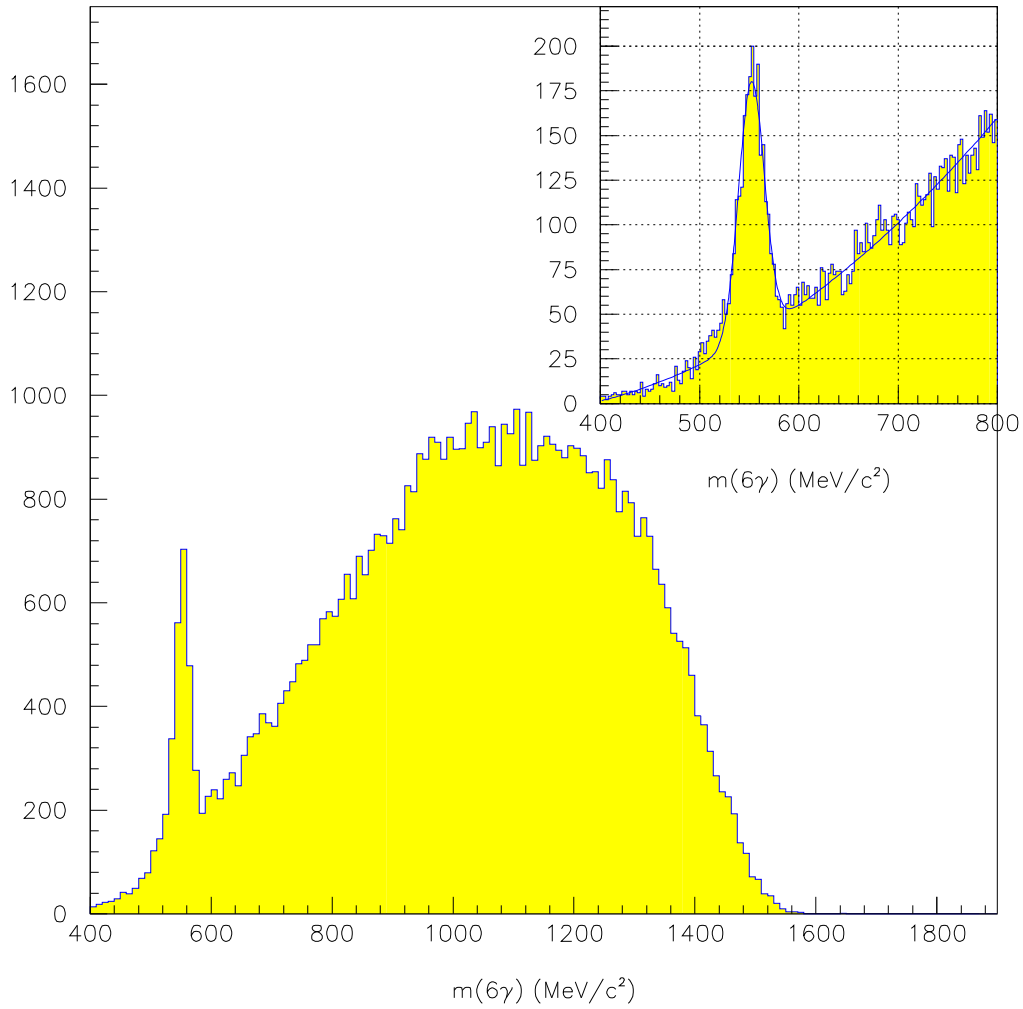

Figure 17: The 6γ invariant mass. The inserted figure has been fit with a gaussian on a quadratic background.

- Exactly one $\pi^+\pi^-\pi^\circ\pi^\circ\pi^\circ$ 3,547 events, (no $\pi^+\pi^-\eta\pi^\circ\pi^\circ$).
- At least one $\pi^+\pi^-\eta\pi^\circ\pi^\circ$ 6 events.
- Exactly one $\pi^+\pi^-\eta\pi^\circ\pi^\circ$ 5 events, (no $\pi^+\pi^-\pi^\circ\pi^\circ\pi^\circ$).

The 7734 events satisfying the 4–C confidence level cut were then used to access the efficeincy of this channel. All events with a 4–C confidence level larger than 25% were examined. The 6γ invariant mass for all of these events is shown in figure 18, the fit to the 6γ spectrum yields:

$$\begin{aligned} A &= 324.7 \pm 7.024 \\ m_\eta &= 553.1 \pm 0.2244 \\ \sigma_\eta &= 13.66 \pm 0.2156 \\ b_0 &= -46.07 \pm 1.166 \\ b_1 &= 0.1753 \pm 0.003793 \\ b_2 &= -0.0001491 \pm 0.00000333 \end{aligned}$$

which when integrated with a bin width of 2.6667, these yield 4169.32 ± 111.65. This yields a nominal efficeincy of

$$\epsilon_{6\gamma} = 0.138977 \pm 0.003722.$$

A similar number can be obtained from the $3\pi^0$ invariant mass. Here we obtain an efficiency of:

$$\epsilon_{3\pi^\circ} = 0.111104 \pm 0.003168.$$

The effects from intermediate resonances are studied in the same fashion as in section 3.1.2 using the $3\pi^0$ invariant mass on a smaller statistical sample. The results are shown in table 8. As before, we define the average as the efficiency, and include the standard deviation from this value as an additional systematic error. This then gives us $\epsilon_{6\gamma} = 0.140127 \pm 0.008173$ and $\epsilon_{3\pi^\circ} = 0.112023 \pm 0.006625$.

Decay Chain	*Generated*	*Accepted*	*Efficiency*
$\eta\pi^+\pi^-$ Phase Space	20000	2297	0.11485 ± 0.0024
$\rho^\circ\eta \rightarrow \eta\pi^+\pi^-$	5003.8	561.54	0.1122
$\eta f_0(975) \rightarrow \eta(\pi^-\pi^+)$	1292.5	148.57	0.1149
$\eta f_2(1270) \rightarrow \eta(\pi^+\pi^-)$	3431.4	433.12	0.1262
$a_0^\pm(980)\pi^\mp \rightarrow (\eta\pi^\pm)\pi^\mp$	3633.6	429.88	0.1183
$a_2(1320)^\pm\pi^\mp \rightarrow (\eta\pi^\pm)\pi^\mp$	7798.5	846.94	0.1086
Average			0.1158 ± 0.0060

Table 8: The efficiency for reconstructing $\eta\pi^+\pi^-$ for the allowed intermediate states.

.

3.3.3 Branching Fraction

We have $N_\eta = 1735.72 \pm 90.98$ events from 6γ and $N_\eta = 1666.89 \pm 72.65$ from $3\pi^\circ$. We take the branching ratio for $\eta \rightarrow 3\pi^0$ as $b_\eta = 0.319 \pm 0.004$ [6]. The total number of $\bar{p}$ stops is $N_{stop} = 3{,}346{,}403 \pm 50{,}915$ (section 2.6), and the efficiency for reconstruction of an η is $\epsilon_{6\gamma} = 0.140127 \pm 0.008173$, $\epsilon_{3\pi^\circ} = 0.112023 \pm 0.006625$. Then the branching ratio, f_b is given as:

$$f_b = \frac{N_\eta}{N_{stop} \cdot b_\eta \cdot \epsilon_\eta}.$$

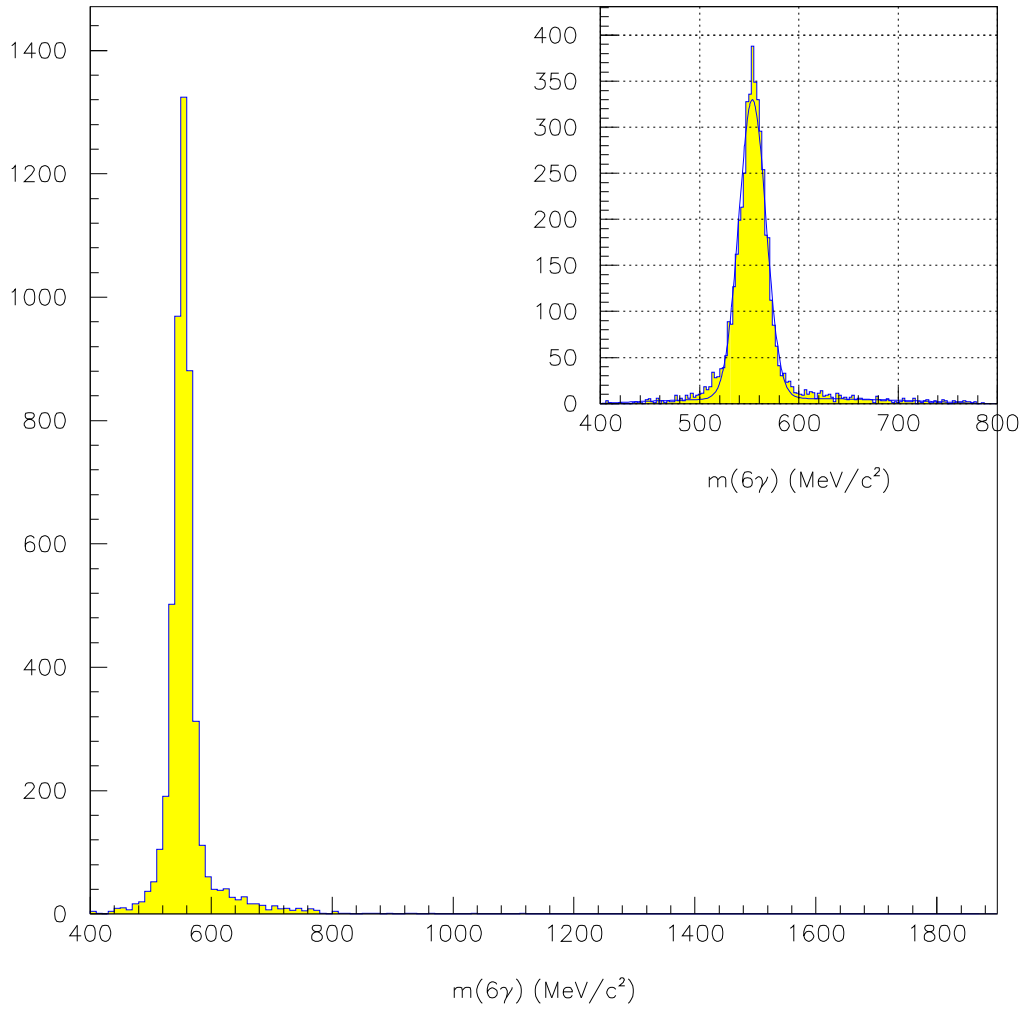

Figure 18: The Monte Carlo 6γ invariant mass. The inserted figure has been fit with a gaussian on a quadratic background.

This gives:

$$BR(\bar{p}p \to \eta\pi^+\pi^-) = (11.60 \pm 0.61 \pm 0.71) \cdot 10^{-3}$$

for 6γ, and

$$BR(\bar{p}p \to \eta\pi^+\pi^-) = (13.94 \pm 0.61 \pm 0.87) \cdot 10^{-3}$$

The first error is statistical and the second is systematic. The fact that these are wildly different gives us some hint that we have encountered problems here.

In order to access the effects of the confidence level cut, the entire analysis was repeated using confidence level cuts of 40% and 60%. These reuslts are shown in table 9. The analysis for $3\pi^0$ was also repeated at various conficence levels. The ratio of accepted events to efficiency for 6γ is a very stable quantity, while that for $3\pi^0$ falls rapidly with an increasing confidence level cut. I have also formed a χ^2 to determine how consistent these reults are. This is shown in the tables, and for the $3\pi^0$, I have formed it from all measurements, and from the last 5 measurements. The value from the last 5 is not unrealistic, $\chi^2/N = 1.7187/5 = 0.3437$, but is three times larger than similar numbers from other channels. In table 10 are computed the branching ratios from the various confidence level cuts. It should be pointed out that the errors are very strongly correlated, so one should be careful in taking averages. However, the simple mean of the last five numbers yields $12.53 \cdot 10^{-3}$, and all of the measurements are consistent with this.

Confidence Level	*Chain*	*Acc. Events*	*M.C. eff.*	*Ratio*
25%	6γ	1735.72 ± 90.98	0.138977 ± 0.003722	12489 ± 735
40%	6γ	1376.42 ± 80.84	0.111976 ± 0.003275	12292 ± 807
60%	6γ	948.09 ± 73.10	0.075918 ± 0.002711	12488 ± 1061
χ^2 for 3 d.f.				0.0381
15%	$3\pi^0$	1666.89 ± 72.65	0.111104 ± 0.003168	15003 ± 781
25%	$3\pi^0$	1411.40 ± 69.85	0.096982 ± 0.002966	14553 ± 847
40%	$3\pi^0$	1072.99 ± 56.71	0.078871 ± 0.002599	13604 ± 847
50%	$3\pi^0$	878.41 ± 51.17	0.064072 ± 0.002294	13706 ± 937
60%	$3\pi^0$	690.65 ± 44.35	0.052005 ± 0.002098	13281 ± 1007
75%	$3\pi^0$	405.16 ± 32.32	0.031601 ± 0.001646	12821 ± 1221
χ^2 for 6 d.f.				3.8361
χ^2 for 5 d.f.				1.7187

Table 9: The number of $\eta\pi^+\pi^-$ as a function of the 7–C confidence level.

Confidence Level	*Branching Ratio*
15%	$(13.94 \pm 0.61 \pm 0.87) \cdot 10^{-3}$
25%	$(13.52 \pm 0.67 \pm 0.86) \cdot 10^{-3}$
40%	$(12.64 \pm 0.67 \pm 0.82) \cdot 10^{-3}$
50%	$(12.73 \pm 0.74 \pm 0.84) \cdot 10^{-3}$
60%	$(12.34 \pm 0.78 \pm 0.84) \cdot 10^{-3}$
75%	$(11.41 \pm 0.91 \pm 0.87) \cdot 10^{-3}$

Table 10: The branching ratio to $\eta\pi^+\pi^-$ as a function of the 7–C confidence level. These are measured using the $\eta \to 3\pi^0$ analysis.

4 Summary

The branching ratio for $\bar{p}p$ into $\omega\pi^0\pi^0$, $\eta\pi^+\pi^-$ and $\eta\pi^0\pi^0$ have been measured in the $\bar{p}p \rightarrow \pi^+\pi^-\pi^0\pi^0\pi^0 \rightarrow \pi^+\pi^-6\gamma$ final state.

$$BR(\bar{p}p \rightarrow \omega\pi^0\pi^0) = (23.98 \pm 0.59 \pm 0.75) \cdot 10^{-3}.$$

This value can be compared with the value from Dombrowski of $(20.8 \pm 1.6) \cdot 10^{-3}$, where the largest uncertainties arise from the all–neutral branching and the decay rate of ω into $\pi^0\gamma$.

$$BR(\bar{p}p \rightarrow \eta\pi^0\pi^0) = (6.10 \pm 0.61 \pm 0.34) \cdot 10^{-3}.$$

This value can be compared to $(9.3 \pm 3) \cdot 10^{-3}$ [8].

$$BR(\bar{p}p \rightarrow \eta\pi^+\pi^-) = (11.60 \pm 0.61 \pm 0.71) \cdot 10^{-3}.$$

$$BR(\bar{p}p \rightarrow \eta\pi^+\pi^-) = (13.94 \pm 0.61 \pm 0.87) \cdot 10^{-3}.$$

This value can be compared to the following other measurements. $(12 \pm 3) \cdot 10^{-3}$ [9], $(12.6 \pm 1.3) \cdot 10^{-3}$ [10] and $(13.7 \pm 1.5) \cdot 10^{-3}$ [11]. About the only conclusions that I am willing to draw are 1: that I have as much scatter in my data as other data and 2: I don't trust these results. I think that the 4–C fit provides the possibility of doing things correctly, but one needs to understand the systematics of it better. I also suspect that an 8–C fit approach would also work. However, I have not done this.

Finally, we can estimate the branching ratio to $\pi^+\pi^-\pi^0\pi^0\pi^0$ from these results. We can make an estimate that the average efficency is about 12.5%. We have seen that this is fairly stable against intermediate resonances. Given 38266 $\pi^+\pi^-\pi^0\pi^0\pi^0$ events, we then get a rough estimate of:

$$BR(\bar{p}p \rightarrow \pi^+\pi^-\pi^0\pi^0\pi^0) = 0.092.$$

References

[1] C. A. Meyer, **User Guide for USDROP, A charged Splitoff Supression Package**, CB–Note 191, (1992).

[2] P. Hidas and G. Pinter, **Kinematic Fitting Software**, CB–Note 138, (1991).

[3] Mark Burchell, **Analysis Writeup on BR($\bar{p}p \rightarrow \pi^+\pi^-$), BR($\bar{p}p \rightarrow K^+K^-$)**, CB–Note 185, (1992), and private communication.

[4] Brigitt Schmid, Proton–Antiproton Annihilation into $\pi^+\pi^-\pi^0\pi^0$ and $\pi^+\pi^-\pi^0\eta$, Ph.D. theis from the University of Zürich, 1991.

[5] S. Dombrowski, **Proton–Antiproton–Annihilation in** $\omega\pi^0\pi^0$, Diplomarbeit, University of Zürich, November (1991).

[6] **Review of Particle Properties, Phys. Rev. D45**, II.6, (1992).

[7] E. Aker, *et. al*, The Crystal Barrel Collaboration, **Phys. Lett. B260**, 249 (1991).

[8] S. Devons, *et. al.*, **Phys. Lett. 47B**, 271, (1973).

[9] C. Baltay, *et. al.*, **Phys. Rev. 145**, 1103, (1966).

[10] M. Foster, *et. al.*, **Nucl. Phys. B8**,174, (1968).

[11] C. Amsler and F. Myhrer, **Annu. Rev. Nucl. Part. Sci. 41**, 219, (1991).